Article

Cell Metabolism

Acceleration of β Cell Aging Determines Diabetes and Senolysis Improves Disease Outcomes

Graphical Abstract

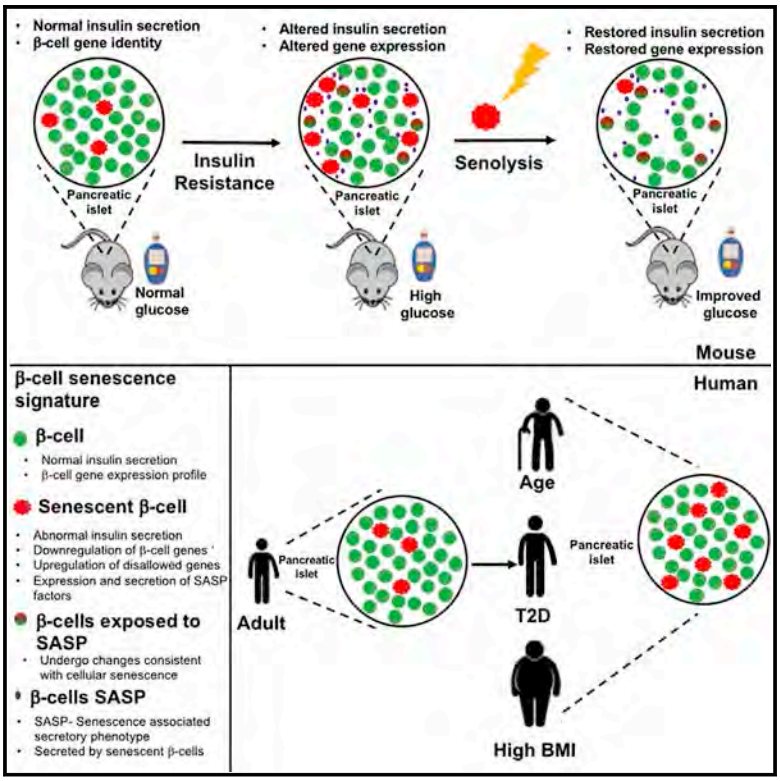

Highlights

- β cell senescence signature reveals loss of identity and upregulation of SASP factors
- Insulin resistance accelerates the appearance of senescent β cells
- Clearance of senescent cells improves glucose levels, β cell function, and identity
- In humans, β cell senescence increases with type 2 diabetes, age, and BMI

Authors

Cristina Aguayo-Mazzucato, Joshua Andle, Terrence B. Lee, Jr., ..., Jan van Deursen, Gordon Weir, Susan Bonner-Weir

Correspondence

cristina.aguayo-mazzucato@joslin.harvard.edu

In Brief

Aguayo-Mazzucato et al. identify the signature of senescent pancreatic β cells and show that the population of senescent β cells is increased by insulin resistance but is partially reversible. Removing senescent cells improves insulin secretion, genetic identity, and glucose homeostasis. These findings provide insight into how β cell senescence contributes to type 2 diabetes, opening new therapeutic targets.

Aguayo-Mazzucato et al., 2019, Cell Metabolism *30*, 1–14
July 2, 2019
https://doi.org/10.1016/j.cmet.2019.05.006

CellPress

Please cite this article in press as: Aguayo-Mazzucato et al., Acceleration of β Cell Aging Determines Diabetes and Senolysis Improves Disease Outcomes, Cell Metabolism (2019), https://doi.org/10.1016/j.cmet.2019.05.006

Cell Metabolism
Article

Acceleration of β Cell Aging Determines Diabetes and Senolysis Improves Disease Outcomes

Cristina Aguayo-Mazzucato,[1,3,*] Joshua Andle,[1] Terrence B. Lee, Jr.,[1] Ayush Midha,[1] Lindsay Talemal,[1] Vaja Chipashvili,[1] Jennifer Hollister-Lock,[1] Jan van Deursen,[2] Gordon Weir,[1] and Susan Bonner-Weir[1]
[1]Joslin Diabetes Center, Harvard Medical School, Boston, MA 02215, USA
[2]Department of Biochemistry and Molecular Biology, Mayo Clinic, Rochester, MN 55905, USA
[3]Lead Contact
*Correspondence: cristina.aguayo-mazzucato@joslin.harvard.edu
https://doi.org/10.1016/j.cmet.2019.05.006

SUMMARY

Type 2 diabetes (T2D) is an age-related disease. Although changes in function and proliferation of aged β cells resemble those preceding the development of diabetes, the contribution of β cell aging and senescence remains unclear. We generated a β cell senescence signature and found that insulin resistance accelerates β cell senescence leading to loss of function and cellular identity and worsening metabolic profile. Senolysis (removal of senescent cells), using either a transgenic INK-ATTAC model or oral ABT263, improved glucose metabolism and β cell function while decreasing expression of markers of aging, senescence, and senescence-associated secretory profile (SASP). Beneficial effects of senolysis were observed in an aging model as well as with insulin resistance induced both pharmacologically (S961) and physiologically (high-fat diet). Human senescent β cells also responded to senolysis, establishing the foundation for translation. These novel findings lay the framework to pursue senolysis of β cells as a preventive and alleviating strategy for T2D.

INTRODUCTION

Type 2 diabetes (T2D) is an age-related disease characterized by a decrease of β cell mass and function, representing a failure to compensate for the high insulin demand of insulin-resistant states (Leahy, 2005; Poitout and Robertson, 2002; Porte, 2001; Prentki et al., 2002; Weir and Bonner-Weir, 2004, 2013). Yet, the role of aging as it pertains to pancreatic β cells is poorly understood, and therapies that target the aging aspect of the disease are virtually non-existent. For many years, β cells can compensate for increased metabolic demands with increased insulin secretion, keeping hyperglycemia at bay. This compensation may be limited by the age-related decline in β cell proliferation seen in rodents (Fan et al., 2011; Rankin and Kushner, 2009; Scaglia et al., 1997; Stolovich-Rain et al., 2012; Teta et al., 2005) and humans (Gregg et al., 2012). This deficiency in proliferative response to increased demand may arise partly from the accumulation of senescent β cells.

Cellular senescence is a state in which cells cease to divide but remain metabolically active with an altered phenotype (Hayflick, 1965; Tchkonia et al., 2013). There are no universal markers of senescence, and the markers that exist are not consistent in every senescent tissue (Campisi and d'Adda di Fagagna, 2007). $p16^{Ink4a}$, a cyclin-dependent kinase inhibitor encoded by the *Cdkn2a* locus, has been identified as both marker and effector of β cell senescence (Krishnamurthy et al., 2006; Krishnamurthy et al., 2004). An increase in $p21^{Cis1}$, another effector of cellular senescence, is thought to mark the entry into early senescence leading to increased $p16^{Ink4a}$ expression, which then maintains senescence, resulting in the expression of the senescence-associated secretory profile (SASP) (Rodier and Campisi, 2011; Stein et al., 1999). SASP profiles differ with tissue type and can include soluble and insoluble factors (chemokines, cytokines, and ECM) that affect surrounding cells and contribute to multiple pathologies (Coppé et al., 2010).

With age, accumulation of dysfunctional senescent β cells likely contributes to impaired glucose tolerance and diabetes. Yet, the specific contribution of β cell aging and senescence to diabetes has received little attention, and the specific SASP profile of β cells remains to be determined.

We have previously found (Aguayo-Mazzucato et al., 2017) that even in young (3–4-month-old) mice, a population of β cells express known aging markers (senescence-associated acidic

Context and Significance

Type 2 diabetes is a disease that increases with age, and defective function of the insulin-producing pancreatic β cells has a decisive role in its development. However, treatments that target the aging component are currently lacking. This work sheds light on the role of β cell aging, or senescence, in the development of diabetes by identifying gene expression changes associated with β cell aging and demonstrating that insulin resistance directly increases the proportion of senescent β cells. Decreasing the number of aged β cells is an effective strategy to restore β cell function and identity and improve glucose metabolism. These results open novel therapeutic approaches against type 2 diabetes.

β-galactosidase activity [β-Gal], *p16^{Ink4a}*, and p53BP1) and that this population increased with age. Aged β cells had impaired function, characterized by higher basal insulin secretion and a lower recruitment to glucose challenges. Moreover, acute insulin resistance, induced by the insulin receptor antagonist S961, resulted in expression of aging markers *p16^{Ink4}* and *Bambi*, suggesting that insulin resistance was a driver of accelerated β cell aging. In the present study, we address the relationship between β cell aging, the development of diabetes, and whether strategies aimed at decreasing the load of aged β cells can improve cellular identity, function, and overall metabolic parameters.

To this end, we developed a β cell senescence signature, which characterizes senescent β cells that actively secrete SASP factors. As hypothesized, metabolic stressors, such as S961-induced insulin resistance and high-fat diet (HFD), accelerated the appearance of aging and senescence markers in β cells and led to their loss of function and impaired glucose tolerance. Clearance of p16^{Ink4a+} cells, using the INK-ATTAC mouse, ameliorated glucose metabolism, improved insulin secretion, and decreased expression of aging, senescence, and SASP genes in islets from models of aging and insulin resistance. Additionally, an oral senolytic compound, ABT263, ameliorated hyperglycemia and improved the β cell gene expression profile in animals challenged with insulin receptor antagonist S961. Human β cells share the same biology: the load of senescent cells increased with age and diabetes, and they overexpress *p16^{Ink4a}*. Our work provides the biological and cellular framework to pursue senolysis of β cells as a potential therapy for inhibiting the progression of T2D.

RESULTS

Senescence and Altered Intercellular Communication Are Main Components of β Cell Aging

Pathway analysis of our previously published microarray data (Aguayo-Mazzucato et al., 2017) comparing β cells from old and young mice revealed that of the 9 described pathways of aging (López-Otín et al., 2013), the old β cells were enriched for genes related to cellular senescence (positive regulation of cell cycle, negative regulation of cell cycle, cell cycle arrest, regulation of mitotic cell cycle) and altered intercellular communication or SASP (cytokine- and chemokine-mediated signaling pathway) (Table S1). Therefore, our focus to understand β cell aging was mostly centered on senescence and its SASP aspect.

A β Cell Senescence Signature Revealed Downregulation of Hallmark β Cell Genes and Expression of "Disallowed" Genes

Pancreatic islets isolated from C57Bl6/J male retired breeders (7–8 months old) were dispersed into single cells and FACS sorted (Figure S1) based on β-Galactosidase (β-Gal) activity as previously described (Aguayo-Mazzucato et al., 2017) (Figure 1A and Figure S1D) and gated for an enriched β cell subpopulation (Figure 1B). β cell enrichment was confirmed using zinc-selective indicator FluoZin-3AM that specifically labels β cells (Figure S1E). To evaluate the potential presence of immune cells in our FACS sorted populations, a sort for CD45$^+$ revealed that about 0.5% of our population were immune cells mainly represented by resident macrophages F4/80$^+$CD11b$^+$ (Figures S1F and S1G) and were distributed within β-Gal$^+$ and β-Gal$^-$ fractions (Figures S1H and S1I). When quantified, our FACS-sorted population was composed of 90% pure β cells and 0.5% resident macrophages (Figure 1C). As is characteristic for senescent cells, β-Gal$^+$ cells were significantly larger than β-Gal$^-$ cells (Figure 1D), and their diameter did not overlap with that of resident macrophages (>20 μm). RNA-seq analysis showed that 3,732 genes out of 15,500 were differentially regulated between β-Gal$^+$ and β-Gal$^-$ β cell samples from the same animals. Importantly, we observed a downregulation of key hallmark β cell identity genes (Subramanian et al., 2005) (Figure 1E), including *Insulin 1*, *Mafa*, *Nkx6.1*, and *Pdx1*. Simultaneously, there was an upregulation of genes whose expression are usually repressed in β cell "disallowed genes" (Pullen et al., 2010; Thorrez et al., 2011), such as *Ldha* and *catalase* (Figure 1F). Specifically curated molecular signature databases (Subramanian et al., 2005) for aging (Figure 1G), and senescence (Figure 1H) genes showed an upregulation of these genes in β-Gal$^+$ as compared to β-Gal$^-$ cells. Using these data, we generated indices for assessment of β cell identity, aging, and senescence (see STAR Methods for specific genes).

Senescent β Cells Actively Produce and Secrete SASP Factors

Analysis revealed an upregulation of SASP genes in the β-Gal$^+$ subpopulation (Figure 2A), and, as part of their SASP profile, primary β cells secreted more IL6, TNF, and CXCL1 than did non-senescent cells (Figure 2B). Conditioned media (CM) generated by collecting media from cultured sorted β-Gal$^+$ and β-Gal$^-$ β cell populations was used to culture dispersed isolated islets. Cells exposed to CM from β-Gal$^+$ cells increased expression of *p16Ink4a* with no change in *p21^{Cis1}* (Figure 2C) compared with those cultured with CM from β-Gal$^-$ cells, suggesting that SASP from senescent primary β cells was functional. Given that β cells are not an inflammatory cell type, and there was potential participation of resident macrophages (<1%), we tested the effect of CM from senescence-induced MIN6 cells, a mouse β cell-immortalized cell line. Senescence was induced by treating these cells with 200 nM doxorubicin or 450 μM H_2O_2 for 24 h and then collecting conditioned media (CM) after 24–48 h to measure SASP protein secretion by a β cell-derived line without contamination by other cell types. Induction of senescence was confirmed by increased expression of *p16^{Ink4a}* and *p21^{Cis1}* mRNA (Figures 2D and 2F); SASP factor proteins were measured in CM showing greater secretion from senescent cells (Figures 2E and 2G). Viability of MIN6 cells was not affected by doxorubicin but was greatly diminished by H_2O_2 (Figure S2).

It is worth noting that the SASP profile differed between primary β cells (Figure 2B) and MIN6 cells (Figures 2E and 2G). This suggests that β cell senescence is a complex stepwise process (as recently suggested by De Cecco et al., 2019) and that more research regarding the timeline and molecular mechanisms behind β cell SASP is needed. To evaluate the correlation between senescence and SASP in a pure β cell model, we knocked down *p16Ink4a* in MIN6 cells using siRNA. A 50% decreased *p16Ink4a* expression resulted in significantly decreased *Il6, Il1a, Igfbp5, Lamb1*, and *Lamc1* mRNA and increased *Cxcl2, Cxcr4, and Ccl2* mRNA (Figure 2H). These data suggest that these factors are downstream of p16Ink4a,

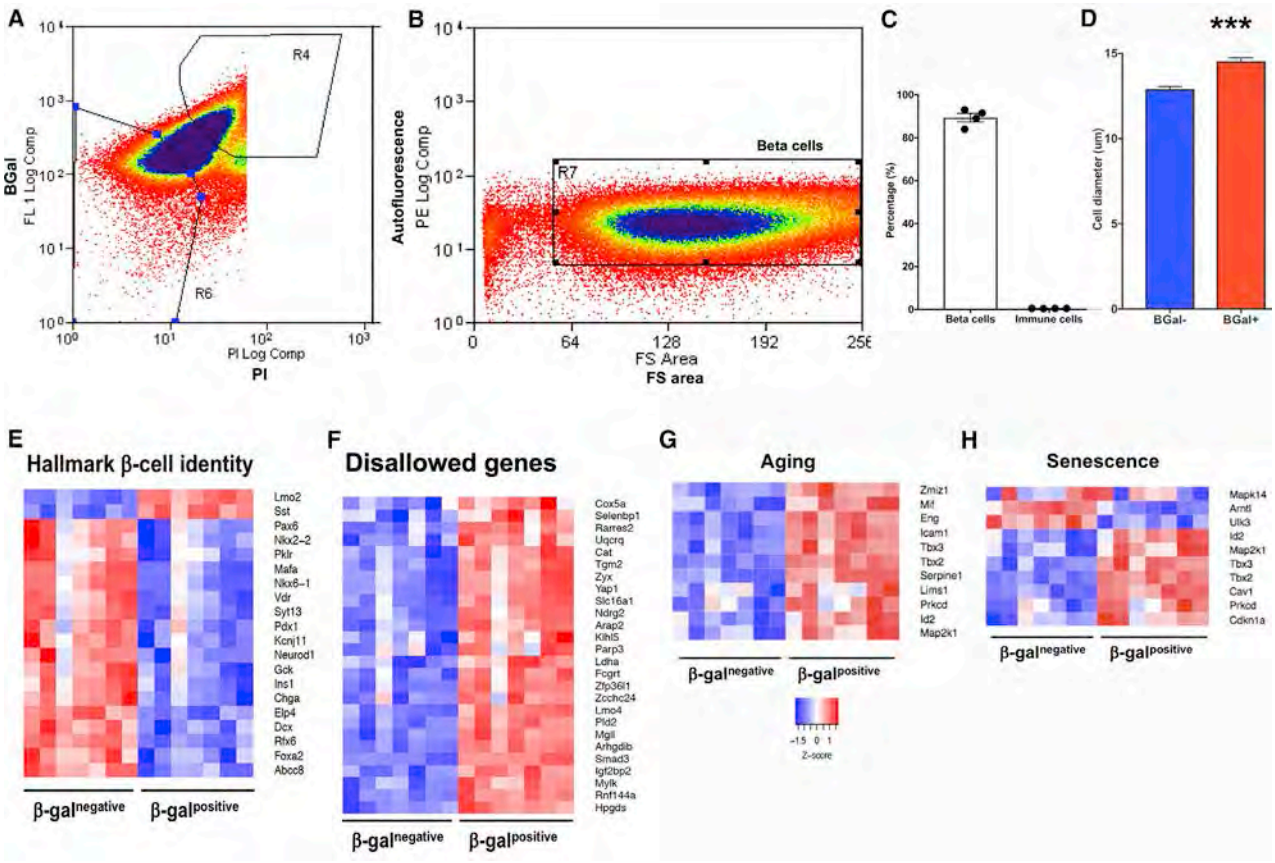

Figure 1. Generation of a β Cell Senescence Signature and Cellular Characteristics

(A and B) Islets isolated from 7–8-month-old C57BL/6J male retired breeders were FACS sorted into non-senescent (β-Gal^{negative}) and senescent (β-Gal^{positive}) subpopulations (A) for RNASeq after gating for enrichment of β cells (B).

(C) Cellular identity of FACS sorted cells was 90% β cells and 0.5% immune cells. Mean ± SEM.

(D) As described for senescent cells, β-Gal^{+} β cells were significantly larger than β-Gal^{-} cells. At least 100 cells were counted from 3 different fields. For RNA-seq data, there were 7 sets of paired samples, each set from islets pooled of 30 mice. Mean ± SEM; $p = 4 \times 10^{-12}$

(E and F) Senescent β cells were characterized by a downregulation of hallmark β cell identity genes (E) and upregulation of disallowed genes (F).

(G and H) Senescent β cells also showed upregulation of specific aging (G) and senescent (H) genes.

although the mechanism of action behind this relationship remains to be determined.

Insulin Resistance Accelerated the Appearance of Senescent β Cells

To study the effects of insulin resistance, we used both the insulin receptor antagonist S961 and high-fat diet (HFD). Both approaches increased the proportion of β-Gal^{+} cells as well as increased the aging and SASP indices of gene expression (Figures 3 and S3A–S3C). First, an acute and severe model of insulin resistance was induced in mice using the insulin receptor antagonist S961 (osmotic minipump administration) that induced marked hyperglycemia and hyperinsulinemia (Figures 3A, 3B, 3H, and 3I). By qPCR and immunostaining, p21^{Cis1} was significantly increased at both the mRNA and protein level (Figures 3F, 3G, and S3). Blood glucose and insulin levels were completely reversed two weeks after removal of the minipumps (Figures 3H and 3I). Interestingly, normalization of hyperglycemia also reversed the aging and SASP indices (Figures 3J, 3K, and S3D), suggesting that cellular senescence is at least partially reversible. After the recovery, β cell-specific genes (comprising the β cell index) were also upregulated, suggesting improved cellular health of β cells.

The second model of insulin resistance used HFD. After 8-week HFD started at 8 weeks of age, body weight and fasting blood glucose levels increased, glucose tolerance deteriorated, as judged by IPGTT (Figures 3M–3O), and peripheral insulin resistance was modestly increased, as determined by an insulin tolerance test (ITT) (Figure S3E), all consistent with a higher demand on the mass and function of pancreatic β cells. Under these conditions, the percentage of β-Gal^{+} cells in dispersed islets increased from 2% to 8% (Figure 3P); additionally, there were significant increases in the aging and SASP indices (Figures 3Q, 3R, and S3B), indicating increased β cell senescence.

Deletion of p16^{Ink4a}-Expressing Cells Improved β Cell Function and Identity

To test whether the deletion of senescent cells had beneficial effects, we tested the 3 models (aging, S961 treatment, and HFD) in INK-ATTAC mice, a whole-body FLAG-tagged transgenic that

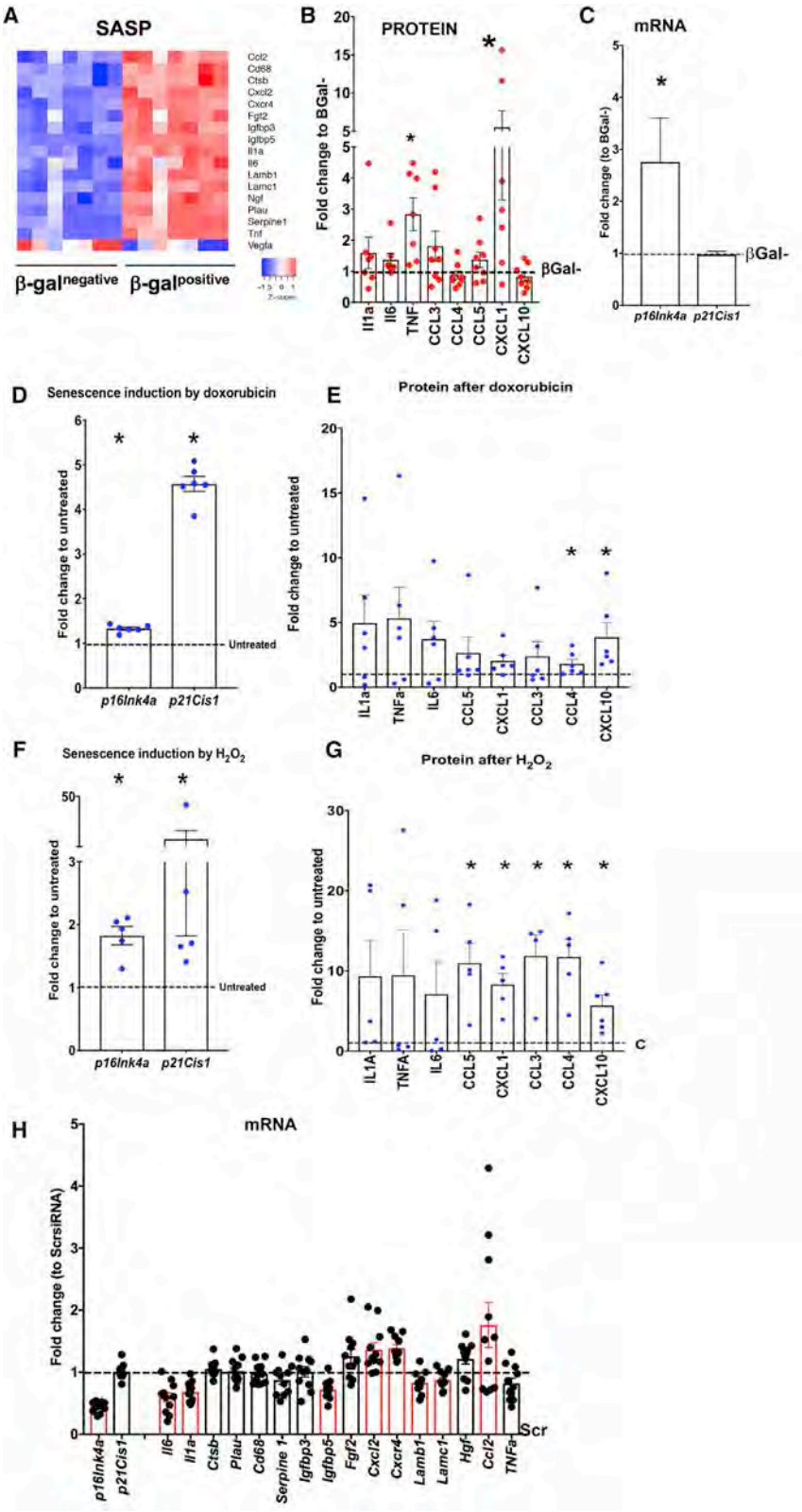

Figure 2. SASP Factors Are Produced and Secreted by Senescent β Cells

(A and B) Senescent β cells were characterized by an upregulation of SASP factors (A), some of which are significantly increased in conditioned media from β-Gal$^+$ cells (B). Each point represents a FACS sorting experiment. Mean concentrations of proteins were IL1a, 6pg/mL; TNFa, 23 pg/mL; IL6, 83 pg/mL; CCL5, 5 pg/mL; CSCL1, 22 pg/mL; CCL3, 6 pg/mL; CCL4, 4 pg/mL; and CXCL10, 2 pg/mL.

(C) Isolated mouse islets that were cultured for 4 days in the presence of CM from β-Gal$^+$ β cells had regulation of *p16^{Ink4a}* compared to those in CM form exposed to CM from β-Gal$^-$ β cells, indicating a functional β cell SASP. CM from 5 FACS sorts were used on 2–3 separate islet isolations.

(D) In immortalized β cell line MIN6 cells, senescence was induced by 24-h exposure to 200 nM doxorubicin; senescence was confirmed by upregulation of *p16^{Ink4a}* and *p21^{Cis1}* mRNA.

(E) Conditioned media from doxorubicin-treated cells had detectable protein levels of several SASP factors compared to non-senescent MIN6 cells. Each point represents an experiment; *p < 0.05.

(F) MIN6 cell senescence was induced by exposing them to 450 μM H_2O_2 for 24 h; senescence was confirmed by upregulation of *p16^{Ink4a}* and *p21^{Cis1}* mRNA.

(G) Conditioned media from H_2O_2-treated cells had detectable protein levels of several SASP factors compared to non-senescent MIN6 cells. Each point represents an experiment; *p < 0.05.

(H) MIN6 cells were treated with *p16^{Ink4a}* siRNA, decreasing expression by 50%. Several SASP factor mRNAs were significantly changed (red bars) compared to cells treated with Scr siRNA, suggesting their regulation in β cells is downstream of *p16^{Ink4a}*. n = 4 experiments in triplicate. Means are plotted with each point representing a single sample. p < 0.05.

Results are mean ± SEM; *p ≤0.05. ttest to control, untreated, or Scr. Wilcoxon test for (B) and (E).

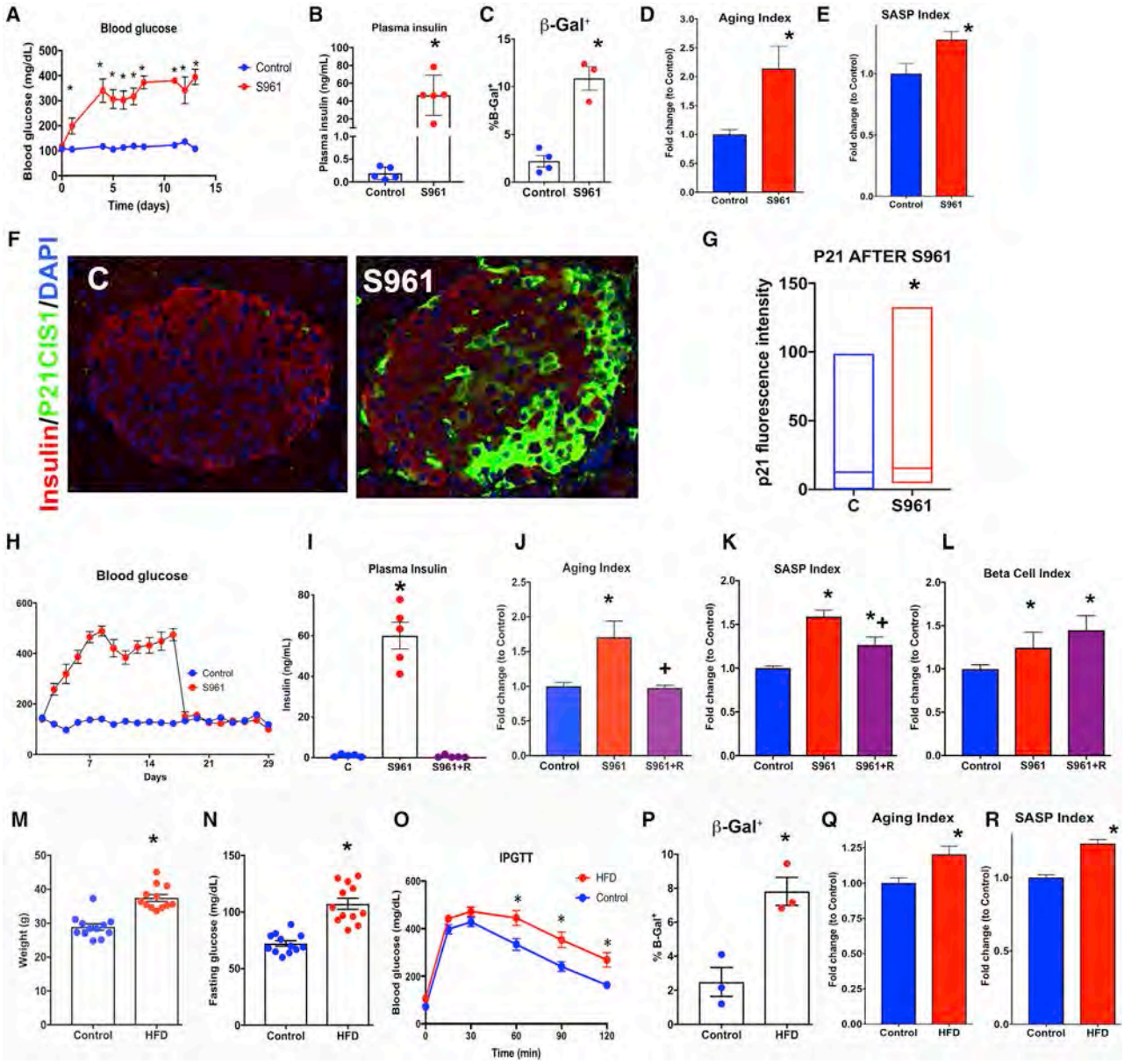

Figure 3. Insulin Resistance Accelerates β Cell Senescence

(A and B) Osmotic minipump administration of the insulin receptor antagonist S961 for 2-week-induced marked hyperglycemia (A) and hyperinsulinemia (B) in 7-month-old male C57Bl6/J mice.

(C–E) Islets from treated mice had a greater proportion of β-Gal$^+$ β cells (C) (12,089–100,000 events/data point) and increased expression of aging (D) and SASP-related (E) genes.

(A–E) 7-month-old male C57Bl6/J; (C) 4-month-old male INK-ATTAC. n = 5 per group; *p < 0.05.

(F) Image of pancreas showing heterogenous colocalization of insulin and P21^{CIS1} in S961-treated animals compared to untreated controls. The magnification bar represents 50 μm.

(G) Quantification of cellular P21^{CIS1} staining intensity presented as mean per β cells of each islet, at least 30 islets counted per pancreas, n = 3 control, 6 S961 animals. Box and violin plot, line at median, *p = 0.02 by Mann-Whitney.

(H–O) Two weeks after minipump excision and normalization of blood glucose (H) and insulin (I) levels, some changes induced by S961 were reversed: both the aging (J) and SASP (K) indices decreased with respect to S961 islets, with no change on β cell-related genes (L) (see Figure S3 for individual values). 7-month-old C57Bl6/J male; n = 5 per group. Eight weeks of high-fat diet (HFD) starting at 8 weeks increased body weight (M), fasting glucose (N), and induced glucose intolerance (O).

(P–R) Islets from treated animals showed a higher proportion of β-Gal$^+$ cells (P) (20,856–40,933 events/data point) and increased aging (Q) and SASP (R) indices. n = 12 C57Bl6/J mice per group; *p < 0.05 with respect to the control diet.

Results are mean ± SEM; *p ≤ 0.05 by t test.

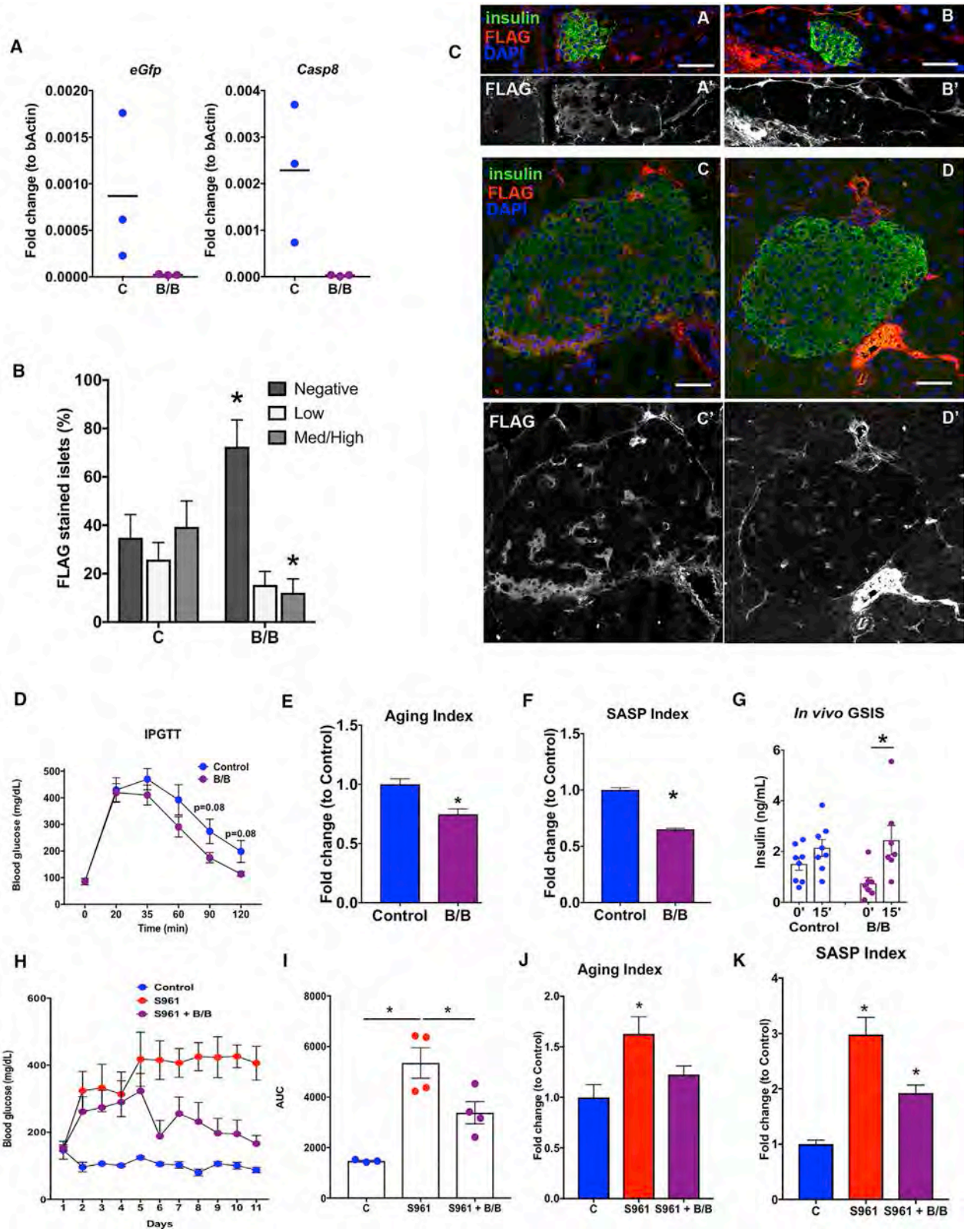

Figure 4. Specific Deletion of p16^{Ink4a}-Expressing Cells Improved Metabolic Profile, β Cell Function, and Gene Expression

(A) Evaluation of deletion protocol with B/B Homodimerizer (10 mg/kg) revealed decreased *eGFP* and *Casp8* mRNA in INK-ATTAC islets. Treatment was two courses of 3 days with 14 days between courses to activate the transgene caspase-8 moiety and lead to cell deletion of p16^{Ink4a}-expressing cells in the INK-ATTAC mice. Each dot represents the islets from an individual animal.

(legend continued on next page)

allows deletion of cells expressing p16^{Ink4a} upon administration of B/B homodimerizer (Baker et al., 2016; Baker et al., 2011). First, we verified that senescent islet cells were deleted after administration of two 3-day courses of B/B homodimerizer (10 mg/kg) with 14 days between courses (Xu et al., 2015) in 1–1.9-year-old animals by measuring eGFP and Caspase 8 levels by qPCR (Figure 4A). At the protein level, this deletion in pancreatic islets was confirmed by staining the pancreas for the transgenic FLAG and insulin (Figures 4B and 4C). Quantification of FLAG staining (Figure 4B) showed a significantly increased proportion of FLAG-negative islets and decreased proportion of those with medium/high FLAG staining after B/B treatment. Then, in aged (1.3–1.6-year-old female) INK-ATTAC mice, treatment with B/B homodimerizer improved β cell aging and SASP indices (Figures 4E, 4F, and S4A) without significant changes in glucose tolerance (Figure 4D). However, β cell function was improved, as seen by *in vivo* GSIS (Figure 4G), which showed decreased basal insulin levels after an overnight fast followed by a significant increase of insulin levels 15 min after a glucose load.

With the second model, acute insulin resistance was induced by S961 over two weeks in 9–14-month-old INK-ATTAC male mice. Two 3-day courses of B/B homodimerizer treatment, separated by 7 days, significantly decreased fed blood glucose levels (Figures 4H and 4I), islet indices for aging, and SASP expression (Figures 4, S4B, and S4C).

Finally, HFD administered to 9-month-old INK-ATTAC mice induced significantly increased body weight and fed glucose levels (Figures 5A and 5B) after 8 weeks, which were blunted by B/B homodimerizer administration in courses of 3 days followed by 14 days in between. After 12 weeks HFD, B/B-treated female INK-ATTAC mice had improved glucose tolerance (Figures 5C and 5D), improved β cell function as reflected by *in vivo* GSIS (Figure 5E), and improved aging and β cell indices, yet an increase in the SASP index (Figures 5F–5H, S5A, and S5B), most likely due to the length of the metabolic stress and induction of irreversible late senescence. The improved genetic changes in β cells induced by B/B senolysis likely explain their improved function.

INK-ATTAC animals are whole-body transgenics, and B/B treatment will have effects in all tissues in which p16^{Ink4a} is expressed, raising the possibility that the improvements in glucose metabolism were due to improved insulin action in fat, liver, and/or muscle. However, the ITTs (which evaluate peripheral insulin resistance) of the treated and untreated groups did not differ but tended to normalization (Figure S5C). Additionally, in peripheral tissues important for glucose homeostasis (fat, liver, and white and red muscle), B/B treatment resulted in no significant changes in *p16^{Ink4a}* and *p21^{Cis1}* mRNA (Figures S5D and S5E). These results underline the importance of β cell senescence in glucose homeostasis and suggest that targeting this cell population is a strategy to consider in diabetes.

A Senolytic Drug, ABT263, Improved Glucose Metabolism and β Cell Identity

Senescent cells have upregulated anti-apoptotic pathways that conserve their presence in otherwise healthy tissues (reviewed in Kirkland et al., 2017). Their deleterious functional effects are then amplified by their secreted SASP that can lead to impairment of neighboring cells. At least 5 senescent cell anti-apoptotic pathways have been identified in different tissues. Senolytic therapies that specifically target these pathways are a promising approach to alleviate some of the conditions associated with an increased load of senescent cells. Based on pathway analysis of our RNASeq data, β-Gal^{+} β cells had upregulation of two of these pathways: the HIF1α pathway (FDR = < 0.0001) that can be targeted with quercetin and dasatinib, and anti-apoptotic members of the BCL2 pathway, such as A1/Bfl1 (FDR < 0.0001) or Mcl1 (FDR < 0.001), that can be targeted with ABT263 (navitoclax). We tested the *in vitro* effects of ABT 263 on sorted β-Gal^{+} and β-Gal^{-} β cells and found that ABT263 killed a significant portion of β-Gal^{+} subpopulation at a dose of 5 μM after 4 days of treatment (Figure 6A). Based on these results, we selected ABT263 for *in vivo* treatment of S961-treated (6–9-month-old) INK-ATTAC male mice. S961-induced insulin-resistant mice that were simultaneously treated with ABT263 had only a 3-fold increase in blood glucose levels, as compared to a 5-fold increase of S961-only-treated mice (Figures 6B and 6C). The load of senescent β cells decreased by 25%, as revealed by β-Gal^{+} FACS sorted population analysis (Figure 6D). When analyzing gene expression, the aging index of islets from ABT263-treated mice did not change compared to the untreated insulin resistant mice, although their *p16^{Ink4a}* levels decreased (Figures S6B and S6E). ABT263 treatment decreased the SASP index of islets but had little effect on aging or β cell indices (Figures 6E–6G, S6A, and S6B). The main caveat of senolytic therapies is that they can act broadly across all cells and tissues. To evaluate which of the main tissues that contributes to glucose metabolism were targeted by the ABT263 treatment, we measured *p16^{Ink4a}* and *p21^{Cis1}* transcripts in islets, liver, white fat, and red and white muscle of treated versus untreated animals. *p16^{Ink4a}* expression decreased only in islets and liver (Figure S6E), while *p21^{Cis1}* was unchanged in all tissues (Figure S6F). ABT263 administration was also tested in an HFD model. 5–6-month-old INK-ATTAC female mice were placed on an HFD for 12 weeks and oral ABT administered during

(B and C) Effects of B/B homodimerizer treatment on deletion of p16^{Ink4a} β cells were evaluated by quantification of FLAG and insulin co-staining. Pancreases from 5-month-old animals (n = 6 per group) were stained in parallel, and confocal pictures were taken under the same settings, such that differences in intensity reflect differences in protein concentration. The magnification bar represents 50 μm; *p < 0.05.

(D–G) Old INK-ATTAC mice partially improved glucose metabolism (D) and recovered β cell function (G) after treatment with B/B homodimerizer. Isolated islets had decreased expression of genes of the aging (E) and SASP (F) indices.

(H and I) 1.3–1.6-year-old INK-ATTAC female mice. n = 7–8 per group; *p < 0.05. INK-ATTAC mice treated with insulin receptor antagonist S961 and B/B homodimerizer had an improved metabolic profile (H), as shown by the AUC of their fed glucose levels (I).

(J and K) Improvement of aging (J) and SASP (K) indices was also observed. 9–14-month-old INK-ATTAC male S961 (20 nM/week) treatment for 2 weeks. n = 3–4 per group; S961 *p < 0.05. (See Figure S4 for individual values.).

Results are mean ± SEM; *p ≤ 0.05.

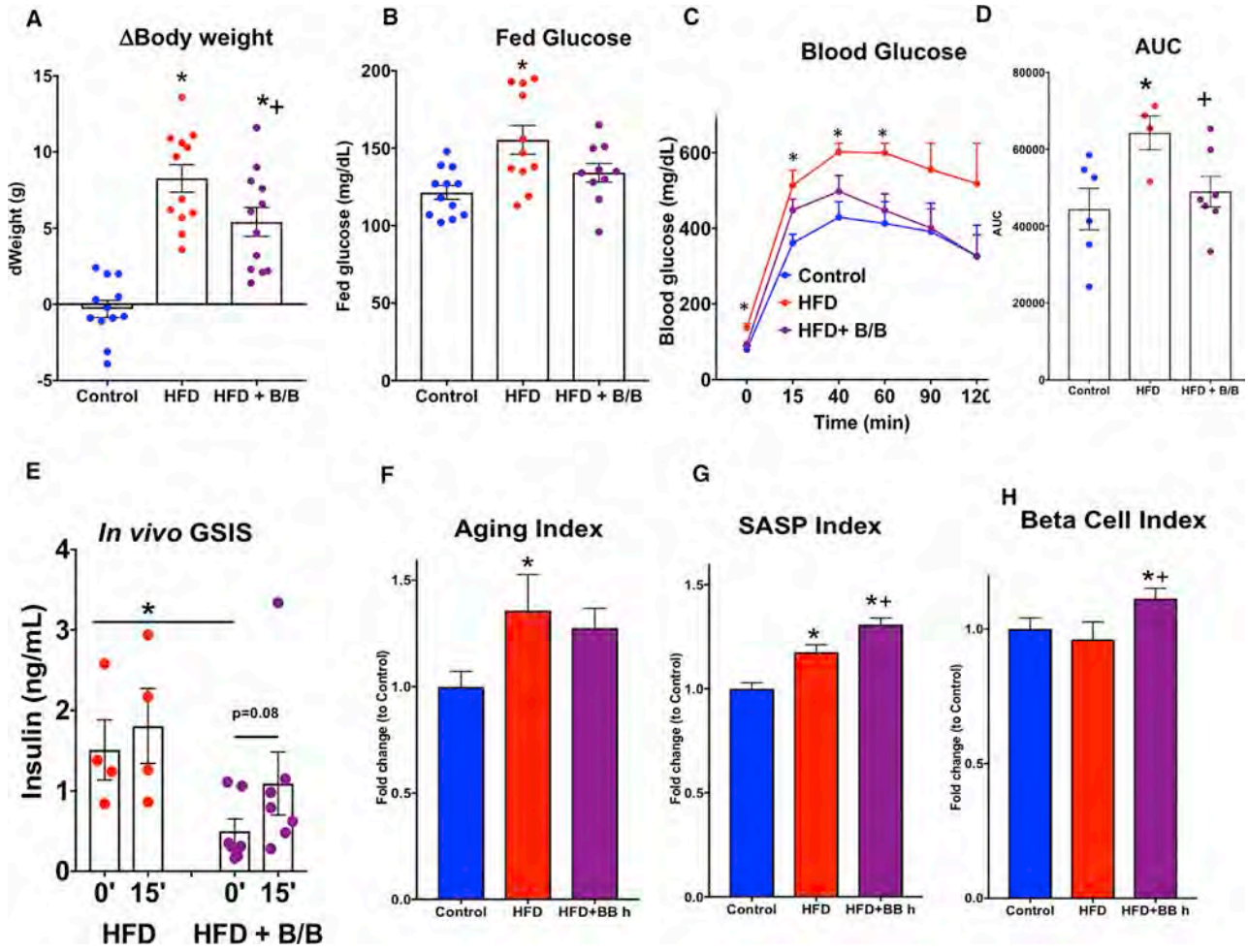

Figure 5. Beneficial Effects of p16^{Ink4a} Deletion in HFD INK-ATTAC Model

(A–D) Changes induced with HFD, such as increased body weight (A), fed hyperglycemia (B), and glucose intolerance (C and D), were blunted after B/B homodimerizer.

(E–H) *In vivo* insulin secretion parameters improved after B/B treatment (E) and although no beneficial changes were seen in aging (F) and SASP (G) indices, islets had an enhanced β cell index (H). (See Figure S5 for individual values.) INK-ATTAC female mice were 9 months old; n = 6–7 animals/group at start of the study; at isolation, 4–7 animals/group remained. *p < 0.05 respect to control; +p < 0.05 with respect to HFD.

Results are mean ± SEM; *p ≤ 0.05.

5-day courses every 3 weeks. Although there were no effects on fed blood glucose (Figure 6H), the percentage of β-Gal$^+$ cells, aging, and SASP indices decreased with respect to the HFD group, with no change in the β cell index (Figures 6I–6K, S6C, and S6D). Their peripheral tissues had significantly decreased *p16^{Ink4a}* (Figure S6G), with only red muscle having significantly decreased *p21^{Cis1}* (Figure S6H). We also tested *in vitro* the effects of quercetin and quercetin + dasatinib on sorted β-Gal$^+$ and β-Gal$^-$ β cells. While quercetin alone did not have effects on senescent β cell mortality (Figure S7A), the combination of quercetin and dasatinib decreased the senescent cell number by 40% (Figure S7B). *In vivo*, acute insulin resistance was induced in mice using S961, and combined quercetin (50 mg/kg) and dasatinib (5 mg/kg) was given orally by gavage once per week. By the end of the two weeks, blood glucose levels decreased in the treated group (Figures S7C and S7D), underlying the physiological value of senolytic therapies in the treatment of diabetes. There were few if any CD45$^+$ immune cells in the islets; this percentage did not change from the 0.5% control values with S961 or senolytic treatment (Figure S7E). These results show that oral administration of a senolytic agent during either acute or chronic insulin resistance was able to partially reverse the adverse metabolic effects as well as provide some restoration of β cell identity.

Translation into Humans

To further our understanding about how these findings translate into human β cell biology, aging, and type 2 diabetes (T2D), we analyzed islets isolated from donors of different ages with and without T2D. As with rodents, the percentage of β-Gal$^+$ islet cells increased in islets isolated from older donors compared to younger ones (Figure 7A), and this proportion seems to be increased further in islets from T2D donors, suggesting that there is a component of β cell senescence in this disease. Furthermore, we confirmed increased expression of *P16^{INK4A}*

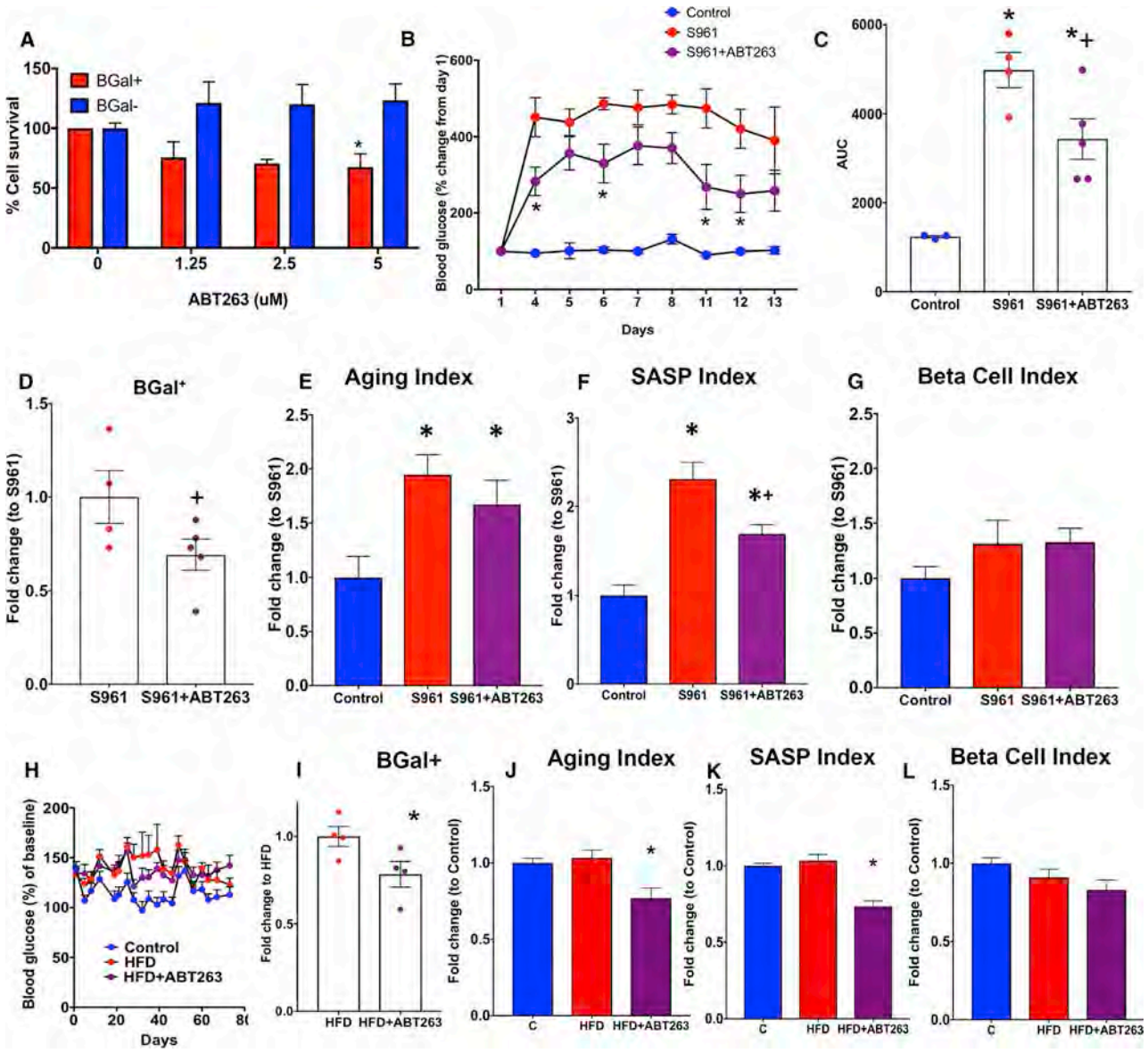

Figure 6. Senolytic Therapies Selectively Killed Senescent Cells and Improved Glucose Metabolism, SASP, and β Cell Indices

(A) ABT263 specifically killed β-Gal$^+$ FACS sorted islet cells *in vitro*. Islets from male retired breeders C57BL/6CRL. n = 2–3 experiments with up to 4 replicates/condition; 4 days.

(B-G) When ABT263 was administered *in vivo* by daily gavage to INK-ATTAC mice treated with S961, circulating blood glucose levels significantly improved (B and C), the percentage of β-Gal$^+$ cells decreased (D) (31,684–64,940 events per data point) with no change in aging index, SASP, and β cell indices (E, F, and G) (see Figure S6 for individual values). INK-ATTAC male mice were 6–9 months old. n = 3–5 animals/group.

(H–L) Administration of ABT263 during 12 weeks of HFD had no effects on fed glucose levels (H) but decreased the percentage of β-Gal$^+$ cells (I) as well as the aging and SASP indices (J and K) and unchanged β cell index (L) compared to those animals receiving HFD without ABT263 treatment (see Figure S6 for individual values). INK-ATTAC 6–9-month-old female mice; n = 3–4 animals/group.

Results are mean ± SEM; *p $\leq$ 0.05.

(Figure 7B) and SASP factors *CCL4* and *IL6* mRNA (Figure 7C) in the β-Gal$^+$ human subpopulation. When human islets were sorted into β-Gal$^+$ and β-Gal$^-$ cells and treated with ABT263, the β-Gal$^+$ subpopulation had a significantly higher cell mortality, as reflected by propidium iodide incorporation (Figure 7D). To further characterize the correlation between β cell aging, senescence, and diabetes, pancreatic sections from different aged donors with and without diabetes were stained for β cell aging marker IGF1R and for DNA damage and senescence marker nuclear P53BP1. In donors younger than 40 years of age, the presence of T2D was associated with a higher intensity of IGF1R in β cells (Figures 7E and 7F), suggesting early aging phenomena associated with diabetes. For P53BP1 (Figure 7G), in non-diabetic donors, there was a direct correlation between nuclear P53BP1 and BMI (Figure 7H), suggesting that states of higher insulin resistance, such as those associated with obesity,

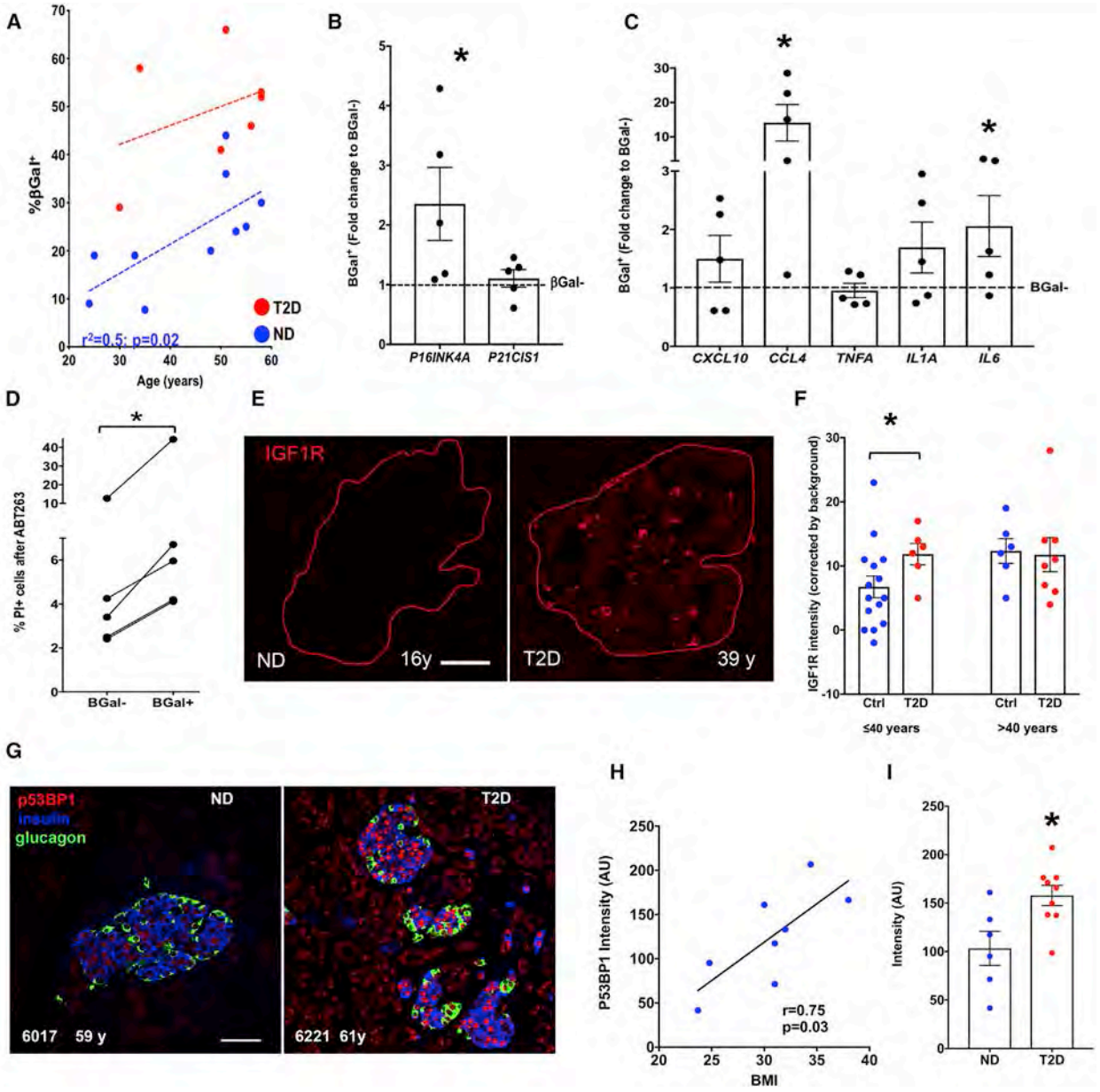

Figure 7. Increased Load of Senescent Human β Cells with Donor Age Associated with Enrichment of *p16^{INK4A}*

(A) The percentage of β-Gal$^+$ cells in human islets increased as the age of the donor increased. Samples from T2D were enriched for senescent cells compared to age-matched non-diabetic donors. Linear regression analysis.

(B) β-Gal$^+$ β cell subpopulation expressed higher levels of *P16^{INK4A}* mRNA than did the β-Gal$^-$ population of the same donor.

(C) mRNA expression levels of SASP factors from human β-Gal$^+$ β cells compared to β-Gal$^-$ cells.

(D) *In vitro* treatment with ABT263 (5 μM) revealed higher cell mortality of β-Gal$^+$ human β cells when compared to β-Gal$^-$ cells from the same donor.

(E) Representative pictures of IGF1R-stained islets in sections of a human pancreas. Sections were stained in parallel and pictures taken in the confocal microscope under the same setting such that differences in intensity reflect differences in protein concentration.

(F) Quantification of IGF1R intensity in islets from donors of different ages, with and without T2D.

(G) Representative pictures of nuclear P53BP1 of human pancreas.

(H) Linear correlation between P53BP1 intensity and BMI in donors without diabetes older than 39 years. Linear regression analysis.

(I) Increased P53BP1 intensity in islets from donors older than 39 years, excluding those with a BMI > 33. Each data point is a separate donor. Magnification bars represent 50 μm.

Results are mean ± SEM; *p ≤ 0.05.

correlated with higher expressions of P53BP1. Finally, when donors with high BMIs (>33) were excluded, an increase in P653BP1 intensity was observed in islets within pancreas from patients with T2D compared with those from non-diabetics (Figure 7I). These results are consistent with our animal models and suggest that human β cells are a potential target for the senolytic

drug therapies in the context of insulin resistance and early diagnosed diabetes.

DISCUSSION

It is widely accepted that T2D has an important aging component; however, no therapies to date have been directed at this aspect. Our work demonstrates that markers of β cell aging and senescence are increased by metabolic stressors of insulin resistance, suggesting that targeting the senescent β cell population may have a therapeutic benefit.

By generating a novel β cell senescence signature, we showed that as they senesce, β cells downregulate expression of key genes vital to their function and identity, such as *insulin, Mafa, Pdx1,* and *Neurod1*. At the same time, the "disallowed," or usually suppressed genes, such as *Ldha*, become expressed, as are genes directly related to both aging and senescence, like $p21^{Cis1}$ and *Igf1r*. This loss of identity in senescent β cells resembles the changes found with glucose toxicity (Jonas et al., 1999).

We show how β cell senescence is a dynamic process that can be accelerated by insulin resistance and be partially reversed. As shown by our S961 experiment, once the induction of insulin resistance is removed and islets allowed to recover for 2 weeks, many of the gene expression changes associated with early senescence reverted toward normal. Given that senescence is a multistep process characterized by the initial upregulation of $p21^{Cis1}$ followed by that of $p16^{Ink4a}$ (De Cecco et al., 2019; Stein et al., 1999) and then SASP factors, our results suggest that some of these initial steps (e.g., $p21^{Cis1}$ increase) might be reversible. However, if the stressor is continued, the senescence program might become irreversible and late senescence SASP factors turned on, as suggested by (De Cecco et al., 2019). Interestingly, some of our models (mainly the acute insulin resistance with S961) showed greater upregulation of $p21^{Cis1}$ than of $p16^{Ink4a}$, suggesting that we might still be within a critical window within which senescence could be reversed if the metabolic stressor were removed. Yet, many cases of insulin resistance and type 2 diabetes are long standing; therefore, interventions aimed at decreasing the load of senescent β cells could be beneficial at various time points, as shown by our aged INK-ATTAC model. When these mice were treated with B/B homodimerizer, their glucose metabolism improved, as did their β cell function and gene profile. Understanding from an aging point of view the changes in gene expression of β cells with insulin resistance and detecting a window of reversibility open up an exciting new therapeutic opportunity to inhibit progression of diabetes.

T2D typically develops in response to over-nutrition and lack of physical activity in subjects with underlying predispositions to insulin resistance and β cell dysfunction. Over time, β cell compensation for the insulin resistance fails, resulting in β cell dysfunction (Leahy, 2005; Porte, 2001; Prentki et al., 2002; Weir and Bonner-Weir, 2004, 2013). As demonstrated in rodents, the mechanisms of compensation for increasing insulin resistance include increased secretion (Weir and Bonner-Weir, 2013) and β cell mass (Brüning et al., 1997). The chronological age of the animals seems to limit the proliferative capacity of β cells (Kushner, 2013), most likely through cellular senescence (Krishnamurthy et al., 2006; Krishnamurthy et al., 2004).

Although cellular senescence has been implicated in the pathophysiology of T2D (Cordisco et al., 2017; Goldstein et al., 1969; Goldstein et al., 1978, 1979), many of these studies focused on the replicative capacity of fibroblasts or senescence markers in endothelial cells. Both may contribute to diabetes complications; however, they are not central to the development of hyperglycemia.

Our results suggest that an acceleration of β cell senescence, representing cellular aging, contributes to the progression of declining glucose metabolism induced by insulin resistance. This was characterized by a decline in islet function as well as an increased expression of senescence, aging genes, and SASP genes. These findings contrast with a study in which 10-day induction of $p16^{Ink4a}$ under the *Ins* or *Pdx1* promoters in β cells of 3–4-week-old transgenic mice resulted in both markers of senescence and improved β cell function (Helman et al., 2016), leading to the conclusion of a novel functional benefit of senescence in β cells. However, β cells of 5–6-week-old mice are not yet fully mature; islets from 3-week-old rats are glucose responsive but lack the robustness found in 2–3-month-old rats (Bliss and Sharp, 1992). Moreover, the fact that $p16^{Ink4a}$ was driven by the insulin or Pdx1 promoter means that the resulting $p16^{Ink4a}$ levels were supraphysiological, which does not necessarily translate into a model of aging or senescence.

Although the population of senescent β cells (β-Gal^{+}) was only 8%–10% in our models, SASP secretion, part of the senescent phenotype, can contribute to multiple pathologies associated with diabetes (Coppé et al., 2010; Thompson et al., 2019). Here, we have characterized a specific SASP profile of β cells and show that some of these factors are detectable in higher concentrations in the conditioned media (CM) obtained from cultured β-Gal^{+} cells than from β-Gal^{-} ones. We also show that these secreted factors were able to upregulate $p16^{Ink4a}$ in islet cells, meaning that the SASP from β cells is functional. Importantly, we saw different SASP profiles between primary rodent and human β cells and with β cell-derived MIN6 cells. This should not be surprising, since, as recently shown by (De Cecco et al., 2019), senescence has a progressive development, and our experiments document cross sectionally the stage of senescence at a given point. In addition, differences may also be due to distinct experimental approaches in our two *in vitro* models. In primary β cells, we observed a correlation between β-Gal activity and SASP expression without any experimental intervention. In MIN6 cells, we sought to identify a causal relationship between senescence-inducing chemicals (H2O2 and doxorubicin) and SASP expression. These chemicals may have also induced other cellular changes that modified SASP expression. Further experiments should be performed to understand the whole senescence process in different models of β cells, and only then will comparisons between models and species be valid.

Senolytic therapies, which specifically target senescent cells, have recently been shown to be beneficial to an array of age-related conditions, such as hepatic steatosis, stem cell biology, and longevity (Chang et al., 2016; Xu et al., 2018). One of the hallmarks of senescent cells is their resistance to apoptosis, and, coupled with their secretion of SASP, they represent a cell population that can induce dysfunction and senescence in their neighboring cells. Using the INK-ATTAC transgenic mouse, we

were able to specifically delete $p16^{Ink4a+}$ cells in models of aging and insulin resistance (S961 and HFD) through the administration of B/B homodimerizer. In all three models, this treatment improved glucose homeostasis, β cell function, and β cell gene expression profile.

One way to target senescent cells is through drugs that focus on upregulated antiapoptotic pathways. At least 5 anti-apoptotic pathways have been described in senescent cells (reviewed in Kirkland et al., 2017). Our RNA-seq data indicated that at least two of these pathways HIF1α and Bcl2 upregulated. We tested drugs specific for each of these two pathways *in vitro*: quercetin and quercetin + dasatinib for HIF1α and ABT263 for Bcl2 pathway. In line with previously published work regarding beneficial effects of quercetin + dasatinib in hepatic steatosis (Ogrodnik et al., 2017), physical function, and lifespan (Xu et al., 2018), quercetin + dasatinib selectively cleared β-Gal$^+$ β cells and improved blood glucose levels in animals treated with S961 without affecting the proportion of immune cells. ABT 263, which has been shown to rejuvenate aged hematopoietic stem cells in mice (Chang et al., 2016), was effective in selectively reducing the percentage of β-Gal$^+$ β cells. When administered *in vivo* in mice with S961 and HFD, ABT263 improved their glucose metabolic profile and β cell genetic identity and specifically reduced $p16^{Ink4a}$ in islets of treated animals. Even though parallel effects were shown by clearing cells with high $p16^{Ink4a}$ expression from INK-ATTAC mice and using senolytics to target an antiapoptotic pathway upregulated in senescence cells, it should be kept in mind that the mechanisms behind these approaches are not the same.

To further the translation potential of our studies into humans, we obtained human islets from donors of different ages and found that β cell senescence load is age dependent, and T2D seems to accelerate this process. Moreover, β-Gal$^+$ human β cells express higher levels of $P16^{INK4A}$ than do the β-Gal$^-$-sorted cells. In mice, ABT263 specifically reduced the load of $p16^{Ink4a}$ transcripts in islets of treated animals, which opens up the possibility that β-Gal$^+$ human cells may respond to senolytic therapies.

The main caveat of senolytic therapies is that they target cells and tissues indiscriminately and broadly. Our model shows that a short-term treatment with ABT263 decreased $p16^{Ink4a}$ *mRNA* only in β cells and liver, while $p21^{Cis1}$ was unchanged in all tested tissues. This should not be surprising since, as previously mentioned, several different antiapoptotic pathways can be upregulated in senescent cells, and which ones are upregulated vary from one tissue to another. Moreover, it has been shown that ABT263 causes apoptosis of senescent endothelial cells but has little effect on senescent fat cell precursors (Zhu et al., 2015); therefore, it might not be expected to have as big an effect on fat tissue as other senolytics. However, in our long-term HFD model, ABT263, decreased levels of $p16^{Ink4a}$ in most peripheral tissues, suggesting that tissue specificity of senolytics might also be achieved by the duration of treatment, with some tissues being more sensitive than others. Identifying cell-specific pathways may render some tissue specificity to senolytic therapies. Moreover, the deletion of senescent cells has been shown to be beneficial for different pathologies, including hepatic steatosis, autoimmune diabetes, hematopoietic stem cells, and longevity; therefore, even if not specific, off-target effects may not represent a clinical problem.

ABT263 was originally tested as a chemotherapeutic agent for its anti-neoplastic effects; however, its oncologic uses are limited by thrombocytopenia (Gandhi et al., 2011; Wilson et al., 2010). While its use as a senolytic agent would necessitate lower and less frequent doses to limit some of its side effects, evaluation of other senolytic compounds with greater potency, specificity, and fewer side effects is necessary. Even so, as a proof of concept, this approach is a potential new therapeutic avenue that should be further explored in diabetes. We believe that β cell senolysis might also be applicable for new onset of autoimmune type 1 diabetes (T1D) where rising blood glucose levels are likely to induce glucotoxicity and lead to loss of β cells (Eisenbarth, 1986), a concept supported by (Thompson et al., 2019). That paper, based on a very aggressive model of autoimmune Type 1 diabetes, the NOD mouse, reveals the presence of a senescent β cell population. Although the pathophysiology of type 1 and type 2 diabetes is very different, both studies support the presence of a β cell senescent subpopulation capable of secreting SASP.

An important consideration in assessing β cell senescence is the potential role of immune cells infiltrating the islets and contributing to the changes in SASP factors and β cell dysfunction and even whether a reduction of these immune cells could be responsible for the beneficial effects of ABT263, which is known to cause neutropenia. To evaluate the potential participation of the immune system, we characterized the presence of immune cells in the islets from the mice we were working with: they represent only 0.5% of the total cell population, while 90% are β cells. Also, the diameters of the β-Gal$^+$ (14 μm) and β-Gal$^-$ (12 μm) cells did not overlap with those of resident macrophages (20–80 μm). Therefore, we believe that the effects we saw were not due to immune cells but were specific to changes in the number and phenotype of the β cells.

In summary, we have established a β cell senescence signature and shown that β cell senescence plays a role in the loss of function and identity, and this process is accelerated by insulin resistance. Using both transgenic and pharmacological senolytic models, we showed that these changes can be delayed and even reversed, leading to a recovery of β cell function and identity. These pathways are preserved in human β cells, opening up a new and exciting approach to address the decline of β cell compensation in T2D.

Limitations of Study

Senescence is a progressive, multistep process that involves the recruitment of different pathways. At this point, the senescence progression in β cells is not fully understood, and neither is it clear which steps along the pathway are reversible if the metabolic stress were removed versus those that are irreversible and can only be targeted through senolytic therapies. As we move forward into understanding the specifics of β cell senescence mechanisms, these points will become clear, as will the most effective interventions at each step. The main caveat of senolytic therapies is that they target cells and tissues indiscriminately and broadly, since they are directed at pathways that can be upregulated in all cell types. However, it would be desirable

to obtain senolytic drugs that have a higher potency when administered orally, such as the one we observed with the transgenic INK-ATTAC model. Hopefully, as companies and groups are actively working to identify potent senolytic compounds with tolerable side effects, the availability of such a drug is feasible in the near future.

STAR★METHODS

Detailed methods are provided in the online version of this paper and include the following:

- KEY RESOURCES TABLE
- CONTACT FOR REAGENT AND RESOURCE SHARING
- EXPERIMENTAL MODELS AND SUBJECT DETAILS
  - Animals
  - Cell Lines
  - Human Tissue
- METHOD DETAILS
  - Assessment of Glucose Homeostasis in Animals
  - Senolytic Treatments
  - Induction of Senescence
  - FACS
  - RNASeq
  - Quantification of Secreted SASP
  - Quantitative Real-Time PCR (QPCR)
  - S961 Treatment
  - Knockdown Experiments
  - Immunostaining and Morphometric Evaluation
- QUANTIFICATION AND STATISTICAL ANALYSIS
- DATA AND SOFTWARE AVAILABILITY

SUPPLEMENTAL INFORMATION

Supplemental Information can be found online at https://doi.org/10.1016/j.cmet.2019.05.006.

ACKNOWLEDGMENTS

We thank Dr. C.R. Kahn for helpful and insightful discussion. Human islets were provided by the NIDDK-funded Integrated Islet Distribution Program (IIDP) at City of Hope, NIH grant no. 2UC4DK098085. Human pancreatic sections were provided by the Joslin Clinical Islet Isolation Core and the Network for Pancreatic Organ Donors with Diabetes (nPOD), a collaborative research project sponsored by JDRF. Organ Procurement Organizations (OPO) partnering with nPOD to provide research resources are listed at https://www.jdrfnpod.org/for-partners/npod-partners. We are grateful to Brooke Sullivan and Aref Ebrahimi for technical and bioinformatic support. This study was supported by grants from the NIH (R01 DK093909 and R01 DK110390, S.B.W.), P30 DK036836 Joslin Diabetes Research Center (DRC Cores: Advanced Microscopy [Chris Cahill], Bioinformatics [Jonathan Dreyfuss and Hui Pan], Flow Cytometry [Angela Wood and Alison Marotta], and Animal Facilities [John Stockton] and P&F to C.A.M.), P30 DK057521 (BADRC P&F to C.A.M.), the Diabetes Research and Wellness Foundation, United States, and an important group of private donors. A.M. was supported through the Harvard College Research Program, Office of Undergraduate Research.

AUTHOR CONTRIBUTIONS

C.A.M. and S.B.W. conceived the project and wrote the manuscript; C.A.M., J.A., T.J.L., A.M., L.T., V.C., and J.H.L. researched data; and G.C.W. provided critical discussions and edited the manuscript. J.V.D. provided critical discussion, animal model, and important reagents. All authors reviewed the manuscript.

DECLARATION OF INTERESTS

The authors declare no competing interests.

Received: October 23, 2018
Revised: February 28, 2019
Accepted: May 1, 2019
Published: May 30, 2019

REFERENCES

Aguayo-Mazzucato, C., van Haaren, M., Mruk, M., Lee, T.B., Jr., Crawford, C., Hollister-Lock, J., Sullivan, B.A., Johnson, J.W., Ebrahimi, A., Dreyfuss, J.M., et al. (2017). Beta cell aging markers have heterogeneous distribution and are induced by insulin resistance. Cell Metab. *25*, 898–910 e895.

Baker, D.J., Wijshake, T., Tchkonia, T., LeBrasseur, N.K., Childs, B.G., van de Sluis, B., Kirkland, J.L., and van Deursen, J.M. (2011). Clearance of p16Ink4a-positive senescent cells delays ageing-associated disorders. Nature *479*, 232–236.

Baker, D.J., Childs, B.G., Durik, M., Wijers, M.E., Sieben, C.J., Zhong, J., Saltness, R.A., Jeganathan, K.B., Verzosa, G.C., Pezeshki, A., et al. (2016). Naturally occurring p16(Ink4a)-positive cells shorten healthy lifespan. Nature *530*, 184–189.

Bliss, C.R., and Sharp, G.W. (1992). Glucose-induced insulin release in islets of young rats: time-dependent potentiation and effects of 2-bromostearate. Am. J. Physiol. *263*, E890–E896.

Brüning, J.C., Winnay, J., Bonner-Weir, S., Taylor, S.I., Accili, D., and Kahn, C.R. (1997). Development of a novel polygenic model of NIDDM in mice heterozygous for IR and IRS-1 null alleles. Cell *88*, 561–572.

Calderon, B., Carrero, J.A., Ferris, S.T., Sojka, D.K., Moore, L., Epelman, S., Murphy, K.M., Yokoyama, W.M., Randolph, G.J., and Unanue, E.R. (2015). The pancreas anatomy conditions the origin and properties of resident macrophages. J. Exp. Med. *212*, 1497–1512.

Campisi, J., and d'Adda di Fagagna, F. (2007). Cellular senescence: when bad things happen to good cells. Nat. Rev. Mol. Cell Biol. *8*, 729–740.

Chang, J., Wang, Y., Shao, L., Laberge, R.M., Demaria, M., Campisi, J., Janakiraman, K., Sharpless, N.E., Ding, S., Feng, W., et al. (2016). Clearance of senescent cells by ABT263 rejuvenates aged hematopoietic stem cells in mice. Nat. Med. *22*, 78–83.

Coppé, J.P., Desprez, P.Y., Krtolica, A., and Campisi, J. (2010). The senescence-associated secretory phenotype: the dark side of tumor suppression. Annu. Rev. Pathol. *5*, 99–118.

Cordisco, S., Magenta, A., Briganti, S., Teson, M., Castiglia, D., Dellambra, E., and Guerra, L. (2017). Accelerated features of senescence in cultured type 2 diabetic skin fibroblasts. Eur. J. Dermatol. *27*, 408–410.

Dai, C., Kayton, N.S., Shostak, A., Poffenberger, G., Cyphert, H.A., Aramandla, R., Thompson, C., Papagiannis, I.G., Emfinger, C., Shiota, M., et al. (2016). Stress-impaired transcription factor expression and insulin secretion in transplanted human islets. J. Clin. Invest. *126*, 1857–1870.

De Cecco, M., Ito, T., Petrashen, A.P., Elias, A.E., Skvir, N.J., Criscione, S.W., Caligiana, A., Brocculi, G., Adney, E.M., Boeke, J.D., et al. (2019). L1 drives IFN in senescent cells and promotes age-associated inflammation. Nature *566*, 73–78.

Eisenbarth, G.S. (1986). Type I diabetes mellitus. A chronic autoimmune disease. N. Engl. J. Med. *314*, 1360–1368.

Fan, R., Kang, Z., He, L., Chan, J., and Xu, G. (2011). Exendin-4 improves blood glucose control in both young and aging normal non-diabetic mice, possible contribution of beta cell independent effects. PLoS ONE *6*, e20443.

Gandhi, L., Camidge, D.R., Ribeiro de Oliveira, M., Bonomi, P., Gandara, D., Khaira, D., Hann, C.L., McKeegan, E.M., Litvinovich, E., Hemken, P.M., et al. (2011). Phase I study of Navitoclax (ABT-263), a novel Bcl-2 family inhibitor, in patients with small-cell lung cancer and other solid tumors. J. Clin. Oncol. *29*, 909–916.

Goldstein, S., Littlefield, J.W., and Soeldner, J.S. (1969). Diabetes mellitus and aging: diminished planting efficiency of cultured human fibroblasts. Proc. Natl. Acad. Sci. USA *64*, 155–160.

Goldstein, S., Moerman, E.J., Soeldner, J.S., Gleason, R.E., and Barnett, D.M. (1978). Chronologic and physiologic age affect replicative life-span of fibroblasts from diabetic, prediabetic, and normal donors. Science *199*, 781–782.

Goldstein, S., Moerman, E.J., Soeldner, J.S., Gleason, R.E., and Barnett, D.M. (1979). Diabetes mellitus and genetic prediabetes. Decreased replicative capacity of cultured skin fibroblasts. J. Clin. Invest. *63*, 358–370.

Gotoh, M., Maki, T., Satomi, S., Porter, J., Bonner-Weir, S., O'Hara, C.J., and Monaco, A.P. (1987). Reproducible high yield of rat islets by stationary in vitro digestion following pancreatic ductal or portal venous collagenase injection. Transplantation *43*, 725–730.

Gregg, B.E., Moore, P.C., Demozay, D., Hall, B.A., Li, M., Husain, A., Wright, A.J., Atkinson, M.A., and Rhodes, C.J. (2012). Formation of a human β-cell population within pancreatic islets is set early in life. J. Clin. Endocrinol. Metab. *97*, 3197–3206.

Subramanian, A., Tamayo, P., et al. (2005). Gene set enrichment analysis. Molecular Signatures Database v6.2. (Broad Institute). PNAS 102, 15545–15550.

Hayflick, L. (1965). The limited in vitro lifetime of human diploid cell strains. Exp. Cell Res. *37*, 614–636.

Helman, A., Klochendler, A., Azazmeh, N., Gabai, Y., Horwitz, E., Anzi, S., Swisa, A., Condiotti, R., Granit, R.Z., Nevo, Y., et al. (2016). p16(Ink4a)-induced senescence of pancreatic beta cells enhances insulin secretion. Nat. Med. *22*, 412–420.

Jonas, J.C., Sharma, A., Hasenkamp, W., Ilkova, H., Patanè, G., Laybutt, R., Bonner-Weir, S., and Weir, G.C. (1999). Chronic hyperglycemia triggers loss of pancreatic beta cell differentiation in an animal model of diabetes. J. Biol. Chem. *274*, 14112–14121.

Kirkland, J.L., Tchkonia, T., Zhu, Y., Niedernhofer, L.J., and Robbins, P.D. (2017). The clinical potential of senolytic drugs. J. Am. Geriatr. Soc. *65*, 2297–2301.

Krishnamurthy, J., Torrice, C., Ramsey, M.R., Kovalev, G.I., Al-Regaiey, K., Su, L., and Sharpless, N.E. (2004). Ink4a/Arf expression is a biomarker of aging. J. Clin. Invest. *114*, 1299–1307.

Krishnamurthy, J., Ramsey, M.R., Ligon, K.L., Torrice, C., Koh, A., Bonner-Weir, S., and Sharpless, N.E. (2006). p16INK4a induces an age-dependent decline in islet regenerative potential. Nature *443*, 453–457.

Kushner, J.A. (2013). The role of aging upon β cell turnover. J. Clin. Invest. *123*, 990–995.

Law, C.W., Chen, Y., Shi, W., and Smyth, G.K. (2014). voom: precision weights unlock linear model analysis tools for RNA-seq read counts. Genome Biol. *15*, R29.

Leahy, J.L. (2005). Pathogenesis of type 2 diabetes mellitus. Arch. Med. Res. *36*, 197–209.

Liao, Y., Smyth, G.K., and Shi, W. (2014). featureCounts: an efficient general purpose program for assigning sequence reads to genomic features. Bioinformatics *30*, 923–930.

López-Otín, C., Blasco, M.A., Partridge, L., Serrano, M., and Kroemer, G. (2013). The hallmarks of aging. Cell *153*, 1194–1217.

Ogrodnik, M., Miwa, S., Tchkonia, T., Tiniakos, D., Wilson, C.L., Lahat, A., Day, C.P., Burt, A., Palmer, A., Anstee, Q.M., et al. (2017). Cellular senescence drives age-dependent hepatic steatosis. Nat. Commun. *8*, 15691.

Poitout, V., and Robertson, R.P. (2002). Minireview: secondary beta-cell failure in type 2 diabetes–a convergence of glucotoxicity and lipotoxicity. Endocrinology *143*, 339–342.

Porte, D., Jr. (2001). Clinical importance of insulin secretion and its interaction with insulin resistance in the treatment of type 2 diabetes mellitus and its complications. Diabetes Metab. Res. Rev. *17*, 181–188.

Prentki, M., Joly, E., El-Assaad, W., and Roduit, R. (2002). Malonyl-CoA signaling, lipid partitioning, and glucolipotoxicity: role in beta-cell adaptation and failure in the etiology of diabetes. Diabetes *51* (*Suppl 3*), S405–S413.

Pullen, T.J., Khan, A.M., Barton, G., Butcher, S.A., Sun, G., and Rutter, G.A. (2010). Identification of genes selectively disallowed in the pancreatic islet. Islets *2*, 89–95.

Rankin, M.M., and Kushner, J.A. (2009). Adaptive beta-cell proliferation is severely restricted with advanced age. Diabetes *58*, 1365–1372.

Ritchie, M.E., Phipson, B., Wu, D., Hu, Y., Law, C.W., Shi, W., and Smyth, G.K. (2015). limma powers differential expression analyses for RNA-sequencing and microarray studies. Nucleic Acids Res. *43*, e47.

Rodier, F., and Campisi, J. (2011). Four faces of cellular senescence. J. Cell Biol. *192*, 547–556.

Scaglia, L., Cahill, C.J., Finegood, D.T., and Bonner-Weir, S. (1997). Apoptosis participates in the remodeling of the endocrine pancreas in the neonatal rat. Endocrinology *138*, 1736–1741.

Schäffer, L., Brand, C.L., Hansen, B.F., Ribel, U., Shaw, A.C., Slaaby, R., and Sturis, J. (2008). A novel high-affinity peptide antagonist to the insulin receptor. Biochem. Biophys. Res. Commun. *376*, 380–383.

Stein, G.H., Drullinger, L.F., Soulard, A., and Dulić, V. (1999). Differential roles for cyclin-dependent kinase inhibitors p21 and p16 in the mechanisms of senescence and differentiation in human fibroblasts. Mol. Cell. Biol. *19*, 2109–2117.

Stolovich-Rain, M., Hija, A., Grimsby, J., Glaser, B., and Dor, Y. (2012). Pancreatic beta cells in very old mice retain capacity for compensatory proliferation. J. Biol. Chem. *287*, 27407–27414.

Tchkonia, T., Zhu, Y., van Deursen, J., Campisi, J., and Kirkland, J.L. (2013). Cellular senescence and the senescent secretory phenotype: therapeutic opportunities. J. Clin. Invest. *123*, 966–972.

Teta, M., Long, S.Y., Wartschow, L.M., Rankin, M.M., and Kushner, J.A. (2005). Very slow turnover of beta-cells in aged adult mice. Diabetes *54*, 2557–2567.

Thompson, P.J., Shah, A., Ntranos, V., Van Gool, F., Atkinson, M., and Bhushan, A. (2019). Targeted elimination of senescent beta cells prevents type 1 diabetes. Cell Metab. https://doi.org/10.1016/j.cmet.2019.01.021.

Thorrez, L., Laudadio, I., Van Deun, K., Quintens, R., Hendrickx, N., Granvik, M., Lemaire, K., Schraenen, A., Van Lommel, L., Lehnert, S., et al. (2011). Tissue-specific disallowance of housekeeping genes: the other face of cell differentiation. Genome Res. *21*, 95–105.

Weir, G.C., and Bonner-Weir, S. (2004). Five stages of evolving beta-cell dysfunction during progression to diabetes. Diabetes *53* (*Suppl 3*), S16–S21.

Weir, G.C., and Bonner-Weir, S. (2013). Islet β cell mass in diabetes and how it relates to function, birth, and death. Ann. N Y Acad. Sci. *1281*, 92–105.

Wilson, W.H., O'Connor, O.A., Czuczman, M.S., LaCasce, A.S., Gerecitano, J.F., Leonard, J.P., Tulpule, A., Dunleavy, K., Xiong, H., Chiu, Y.L., et al. (2010). Navitoclax, a targeted high-affinity inhibitor of BCL-2, in lymphoid malignancies: a phase 1 dose-escalation study of safety, pharmacokinetics, pharmacodynamics, and antitumour activity. Lancet Oncol. *11*, 1149–1159.

Wu, D., Lim, E., Vaillant, F., Asselin-Labat, M.L., Visvader, J.E., and Smyth, G.K. (2010). ROAST: rotation gene set tests for complex microarray experiments. Bioinformatics *26*, 2176–2182.

Xu, M., Palmer, A.K., Ding, H., Weivoda, M.M., Pirtskhalava, T., White, T.A., Sepe, A., Johnson, K.O., Stout, M.B., Giorgadze, N., et al. (2015). Targeting senescent cells enhances adipogenesis and metabolic function in old age. eLife *4*, e12997.

Xu, M., Pirtskhalava, T., Farr, J.N., Weigand, B.M., Palmer, A.K., Weivoda, M.M., Inman, C.L., Ogrodnik, M.B., Hachfeld, C.M., Fraser, D.G., et al. (2018). Senolytics improve physical function and increase lifespan in old age. Nat. Med. *24*, 1246–1256.

Zhu, Y., Tchkonia, T., Pirtskhalava, T., Gower, A.C., Ding, H., Giorgadze, N., Palmer, A.K., Ikeno, Y., Hubbard, G.B., Lenburg, M., et al. (2015). The Achilles' heel of senescent cells: from transcriptome to senolytic drugs. Aging Cell *14*, 644–658.

STAR★METHODS

KEY RESOURCES TABLE

REAGENT or RESOURCE	SOURCE	IDENTIFIER
Antibodies		
See Table S4 for information of antibodies used for staining and FACS	This paper	N/A
Biological Samples		
See Table S2 for donor information on human pancreatic samples	This paper	N/A
Chemicals, Peptides, and Recombinant Proteins		
S961 was a generous gift from Dr. Lauge Schaffer	Novo Nordisk, Denmark	N/A
B/B homodimerizer	Dr. Jan van Deursen, Mayo Clinic	N/A
B/B homodimerizer	Clontech	635069
ABT263	Selleck Chemicals	S1001
Quercetin,> = 95% (HPLC), solid	Sigma-Aldrich	Q4951-10G
D-3307 Dasatinib, Free Base, > 99%	LC Laboratories	302962-49-8
Fast Sybr Green Master Mix	Fisher Scientific	43-856-17
Critical Commercial Assays		
Cellular Senescence Live Cell Analysis Assay Kit (SA-β-gal, Fluorometric)	Enzo Life Sciences	enz-kit 130-0010
STELLUX® Chemi Rodent Insulin ELISA Jumbo	Alpco	80-INSMR-CH10
PicoPure™ RNA Isolation Kit	ThermoFisher Scientific	kit0204
LEGENDplex™ Mouse IL-1α Capture Bead A5, 13X 100 tests (270 ul)	BioLegend	740152
LEGENDplex™ Mouse IL-6 Capture Bead B4, 13X 100 tests (270 ul)	BioLegend	740159
LEGENDplex™ Mouse CCL5 (RANTES) Capture Bead A4, 13X 100 tests (270 ul)	BioLegend	740092
LEGENDplex™ Mouse CCL3 (MIP-1α) Capture Bead B4, 13X 100 tests (270 ul)	BioLegend	740090
LEGENDplex™ Mouse CCL4 (MIP-1β) Capture Bead B5, 13X 100 tests (270 ul)	BioLegend	740091
LEGENDplex™ Mouse CXCL10 (IP-10) Capture Bead B3, 13X 100 tests (270 ul)	BioLegend	740100
LEGENDplex™ Mouse Inflammation Panel Standard 1 vial	BioLegend	740371
LEGENDplex™ Mouse CXCL1 (KC) Capture Bead A8, 13X 100 tests (270 ul)	BioLegend	740096
LEGENDplex™ Mouse Proinflammatory Chemokine Detection Antibodies 100 tests (3.5 ml)	BioLegend	740074
LEGENDplex™ Mouse Proinflammatory Chemokine Standard 1 vial	BioLegend	740370
LEGENDplex™ Mouse Inflammation Panel Detection Antibodies 100 tests (3.5 ml)	BioLegend	740165
LEGENDplex™ Mouse TNF-α Capture Bead A7, 13X 100 tests (270 ul)	BioLegend	740154
LEGENDplex™ Mouse IL-6 Capture Bead B4, 13X 100 tests (270 ul)	BioLegend	740159
LEGENDplex™ Mouse IL-1α Capture Bead A5, 13X 100 tests (270 ul)	BioLegend	740152
LEGENDplex™ Mouse Inflammation Panel (13-plex) with V-bottom Plate 100 tests	BioLegend	740446

(*Continued on next page*)

Continued

REAGENT or RESOURCE	SOURCE	IDENTIFIER
LEGENDplex™ Buffer Set A 100 tests	BioLegend	740368
LEGENDplex™ Buffer Set B 100 tests	BioLegend	740373
V-bottom Plate for LEGENDplex™ Assay 1 plate	BioLegend	740379
MicroAmp® Optical 384-Well Reaction Plate with Barcode	Thermo Fisher Scientific	4309849
SMARTpool: ON-TARGET plus Cdkn2a siRNA	Dharmacon	L-043107-00-0005
ON-TARGET plus non-targeting pool	Dharmacon	D-00810-10-05
Deposited Data		
RNASeq data	This paper	GSE121539
Experimental Models: Organisms/Strains		
C57/Bl6J mice	Jackson	000664
INK-ATTAC mice	Dr. Jan van Deursen, Mayo Clinic	N/A
Oligonucleotides		
See Table S3 for qPCR primers	This paper	N/A
Software and Algorithms		
Prism 7 software	GraphPad software	https://www.graphpad.com/scientific-software/prism/

CONTACT FOR REAGENT AND RESOURCE SHARING

Further information and requests for resources and reagents should be directed to and will be fulfilled by the Lead Contact, Dr. Cristina Aguayo-Mazzucato (cristina.aguayo-mazzucato@joslin.harvard.edu).

EXPERIMENTAL MODELS AND SUBJECT DETAILS

Animals

All experiments were conducted at Joslin Diabetes Center with approval of its Animal Care and Use Committee; mice were kept on a conventional facility in a 12-hour light/dark cycle with water and food *ad libitum,* with a temperature between 22.2-22.7°C. When specified, DIO very high fat diet (VHFD) 60kcal% fat (Fisher Scientific) was used for the specified amount of time. C57Bl6/J mice were acquired from Jackson Labs. Breeding pairs of INK-ATTAC mice (C57BL/6) were the gift of Dr. Jan van Deursen (Baker et al., 2011) and all the animals used came from our colony. Both male and female mice were used except when noted.

Cell Lines

For induction of senescence models and transfection experiments murine β cell line MIN6 cells were used and maintained in high-glucose Dulbecco's modified Eagle's medium (DMEM-H) supplemented with 15% FBS and 0.05% b-Mercaptoethanol (99% Cell culture tested) at 37°C, 5% CO_2. These were originally received from Dr. Jun-ichi Miyazaki, Osaka University Medical School and the sex of the cell line is not available.

Human Tissue

Pancreases from adult brain-dead donors were provided by the NIDDK-funded Integrated Islet Distribution Program (IIDP) at City of Hope. Upon arrival, islets were cultured in CMRL media 5.5 mM glucose complemented with 10% FBS, 1% Glutamax, 1% Pen/Strep. After overnight culture, islets were dispersed into single cells using 0.25% Trypsin-EDTA for 15 min at 37°C. Single cells were then FACS-sorted based on acidic β-Gal activity (Aguayo-Mazzucato et al., 2017). Additionally paraformaldehyde fixed paraffin pancreatic sections of donor human pancreas were obtained through nPOD and from the Joslin Clinical Islet Isolation core for immunostaining. All tissues were approved for research and had IRB exempt status and we used the samples of suitable donors (in terms of age and diabetes status) that became available from IIDP, Joslin and NPOD. Details of donors are given in Table S2.

METHOD DETAILS

Assessment of Glucose Homeostasis in Animals

Body weight and morning fed glucose levels were monitored longitudinally. Blood glucose values were measured using a Contour glucometer (Bayer) on blood from tail snip. For intraperitoneal glucose tolerance tests, blood samples from mice fasted overnight (15 h) were collected at 0, 15, 30, 60, 90, and 120 min after an intraperitoneal injection of glucose (2 g/kg body weight). For *in vivo*

GSIS, the insulin was measured from serum collected at the 0 and 15 min time points of the IPGTT. Concentrations were determined using the Alpco Stellux rodent insulin ELISA kit (NH). For insulin tolerance tests, mice were fasted for 4 h, insulin (Humulin R; Eli Lilly, Indianapolis, IN; 0.5 units/kg body weight) injected intraperitoneally, and blood glucose measured at 0, 15, 30, and 60 min.

Under anesthesia, pancreas was excised for either fixation in 4% (para)-formaldehyde (PFA) for 2h and embedded in paraffin for histology or islets isolated by collagenase digestion (Gotoh et al., 1987) and handpicked for RNA or FACS sorting. Briefly, isolation of pancreatic islets was done after a pancreatic ductal injection of collagenase followed by a stationary *in vitro* digestion for 18 min in a 37oC waterbath. After the reaction was stopped, islets were isolated using a Ficoll gradient followed by centrifugation. The tissue in the interface was collected, washed, sedimented and handpicked for purity.

Senolytic Treatments

The deletion protocol of $p16^{Ink4a}$-expressing cells for INK ATTAC mice consisted in the administration of two 3-day courses of B/B homodimerizer (10mg/kg) or with 7-14 days in between courses to activate the caspase-8 moiety. *In vitro*. A dose response kill curve for ABT263 and for quercetin, quercetin (50 μM) + dasatinib (250 nM) were used on FACS sorted β-Gal^+ and β-Gal^- cells for 4 days. Cell viability was evaluated after trypsinizing the cells and quantifying propidium iodine negative cells on MACSQuant. *In vivo*. Mice were treated with vehicle (DMSO:polyethylene glycol 400:Phosal 50 PG At 10:30:60) or ABT263 (Selleck Chemicals, in ethanol:polyethylene glycol 400:Phosal 50 PG). ABT263 was administered to mice by gavage at 50 mg/ kg body weight per day (mg/kg/d) for 4-5 d per cycle, with a week between the cycles. DQ was administered orally by gavage once per week at a dose 5mg/kg dasatinib, 50mg/kg quercetin.

Induction of Senescence

MIN6 cells were treated with 200 nM of doxorubicin or 450 μM of H2O2 in DMEM media for 24h. Doxorubicin or H2O2 was removed and media was replaced with DMEM-H, 15% charcoal-stripped FBS, 0.05% β-Mercaptoethanol (99% Cell culture tested), and 1% Penicillin-Streptomycin for 24h to generate conditioned media (CM).

FACS

Isolated rodent or human islets were dispersed using 0.25% Trypsin-EDTA for 15 min at 37°C and were resuspended in FACS buffer (2% fetal bovine serum (FBS) (Cellgro, Manassas, VA) in PBS). Using a DakoCytomation MoFlo Cytometer (Dako, Ft. Collins, CO) or Aria (BD FACS Aria IIu and BD FACS Aria Special Order Research Product), cells were gated according to forward scatter and the percentage of β cells by insulin staining ranged from 80%–90%. Propidium iodide was used to exclude dead cells. For sorting based on acidic β-Gal activity, a fluorescent substrate was used (Enzo Life Sciences enz-kit 130-0010) following the manufacturer's instructions; incubation time with the substrate was optimized at 37°C for 1h in rodents and 2h in humans. β-Gal^+ and β-Gal^- subpopulations were either collected for RNA extraction or plated in previously 804 g treated wells and used for staining, analysis of SASP, or evaluation of response to senolytic therapies. For evaluation of cellular composition, zinc -selective indicator FluoZin-3 AM was used as specified by the manufacturer to evaluate the β cell subpopulations. To detect immune cells, dispersed islets were blocked during 45 min with a Blocking solution of PBS-CMF, 2% FBS, 1% rat normal serum, 1% goat normal serum followed by an incubation of 30 min at 4°C in the presence of anti-CD45, anti-F4/80 and anti-CD11b antibodies (Table S4) (Calderon et al., 2015). Cells were then washed (PBS-CMF 2% FBS) and analyzed in FACS buffer. Our full FACS gating strategy can be seen in Figure S1.

RNASeq

β cells from dispersed islets of 7-8 month old male C57BL/6J mice were FACS sorted based on acidic β-galactosidase activity into β-Gal + and β-Gal^- populations, and RNA extracted using PicoPure Arcturus kit. Seven sets of paired samples each from islets pooled from 30 mice were used for RNaseq. Gene expression profiles using HiSeq v4 SE50 250 mil reads by Hudson Alpha Institute for Biotechnology (Huntsville, AL). Reads were aligned to the mouse genome (GRCm38) using Subread aligner and counted with featureCounts v 1.5.2 (Liao et al., 2014). Read counts were transformed to log2-counts per million (LogCPM), their mean-variance relationship was estimated, their weights were computed with voom (Law et al., 2014), and their differential expression was assessed using linear modeling with the R package limma (Ritchie et al., 2015). P values were corrected using the Benjamini-Hochberg false discovery rate (FDR). Gene sets based on canonical pathways, ChIP Enrichment Analysis, and Targetscan conserved miRNA targets were tested using the limma Roast method (Wu et al., 2010).

Quantification of Secreted SASP

Mouse β cells FACS-sorted for β-Gal activity were plated in 100 μL of media (RPMI + 10% FBS + 1% Penicillin-Streptomycin). After 24 hours, the media was replaced with 100 μL of charcoal-stripped media (RPMI + 10% Charcoal-Stripped FBS + 1% Penicillin-Streptomycin) and cultured for another 24 hours to produce conditioned media (CM) for analysis of secreted factors. CM for each well of cultured β cells was collected and analyzed using LEGENDPlex (Biolegend) selected panels for Mouse Inflammatory Factors and Mouse Proinflammatory Chemokines. LEGENDPlex panels measure the concentration of candidate proteins using a bead-based immunoassay. In the assay, capture beads are mixed into the CM, and specific antibodies on the beads bind to target proteins. The addition of detection antibodies and streptavidin-phycoerythrin produces unique fluorescent signal for each target protein with signal intensities proportional to the protein concentration. Those fluorescent signals were measured using MACSQuant and

FACSAria machines. For transfer experiments, β-Gal$^+$ and β-Gal$^-$ cells were plated in a 96-plate and cultured in the presence of charcoal-stripped media for 48 h. CM was then collected and transferred to dispersed and plated dispersed islet cells during 4 days. At the end, cells were picked up, RNA extracted and used for qPCR quantification.

Quantitative Real-Time PCR (QPCR)

Total RNA isolated with PicoRNA extraction kit (Arcturus) or RNEasy Plus Mini Kit (QIAGEN) was reverse transcribed (SuperScript reverse transcriptase, Invitrogen). QPCR used SYBR green detection and specific primers (Table S3). Samples were normalized to β-actin for mouse and TBP for human, and the comparative CT (threshold cycle) method used to calculate gene expression levels. We generated indices for presentation of the PCR data: Aging index: mean of normalized values of *p16^{Ink4a}*, *p21^{Cis1}*, *Bambi* and *Igf1r.* SASP Index: Mean of normalized values *Il6, Il1a, Ctsb, Plau, Cd68, Serpine 1, Igfbp3, Igfbp5, Fgf2, Cxcl2, Cxcr4, Lamb1, Lamc1, Hgf, Ccl2, TNFα*. β cell Index: Mean of normalized values of *Ins1, Mafa, Pdx1, Neurod1, Nkx6.1, Gck.*

S961 Treatment

S961 was a generous gift from Dr. Lauge Schaffer (Novo Nordisk) (Schäffer et al., 2008). Vehicle (PBS or NaCl 0.9%) or 20 nmol S961 was loaded into Alzet osmotic pump 2001 and implanted subcutaneously on the back of mice (Dai et al., 2016) and changed weekly for a total of two weeks.

Knockdown Experiments

As previously published (Aguayo-Mazzucato et al., 2017) siRNA against mouse *p16^{Ink4a}* and RNA interference-negative control were purchased from Thermo Scientific/Dharmacon (Lafayette, CO). MIN6 cells were transfected using DharmaFECT following manufacturers' instructions. After 48 h transfection, the cells were harvested for RNA and qPCR analysis. Results are presented as fold change to MIN6 cells treated with nonspecific siRNA (siScr).

Immunostaining and Morphometric Evaluation

Paraffin sections were deparaffinized with ethanol gradients, washed with PBS and antigen retrieval with citric acid was done for P21, P53BP1 and IGF1R. For FLAG, permeabilization was done with a Triton X 0.3% solution. After washing with PBS + 1% NDS, slides were incubated overnight with primary antibody (Table S4). This was followed by subsequent washes and incubations for 1h with secondary antibodies that were coupled to Cy3, FITC, Cy5, Texas Red, and DAPI for nuclear staining. For P21 staining, TSA amplification was used. For quantification, islet images were captured systematically covering the whole section in confocal mode on a Zeiss LSM 710 microscope. Every cluster of insulin-stained cells (3-7 cells) or islet (8 or more cells)/section was evaluated; sections were coded and read blindly. For each age, 3-4 animals were evaluated. For human samples, sections from one block from the body of the pancreas from donors as listed in Table S2. Immunostaining processing and imaging were done in parallel and using the same confocal settings for each antigen such that differences in intensity reflect the differences in protein.

QUANTIFICATION AND STATISTICAL ANALYSIS

Data are shown as mean ± SEM. For statistical analysis, unpaired Student's t tests were used to compare two groups, and one-way ANOVA followed by post hoc test for more than two groups. Normality analysis was performed and non parametric statistics were run when samples did not meet the criteria for normal distribution. A p value < 0.05 was considered significant. Prism software was used for graphs and statistical analysis (significance and distribution). Animals were assigned to either control, intervention or treatment groups depending on their age and gender to have equal distribution among all groups. In the case of INK ATTAC animals, their genotype was used to determine which animals would be in the B/B homodimerizer group, trying to have an equal representation in the vehicle treated groups.

Processing of samples for qPCR, slides and image quantification were done in a blind manner. The sample size was a minimum of 3 per group and was determined by the number of animals in the colony of a determined age and gender.

Animals were excluded from the analysis if they became sick or developed physical anomalies. Data outliers were determined using Grubbs outlier test or deviating more than 2 standard deviations from the mean (unless they were determined to not follow a normal distribution).

DATA AND SOFTWARE AVAILABILITY

The accession number for the genomic data reported in this paper is GSE121539.